


AUTHOR QUERY FORM

	Book: ZARKO-9780128027103 Chapter: 11	Please e-mail your responses and any corrections to: E-mail: A.Sivaraj@elsevier.com
---	--	--

Dear Author,

Any queries or remarks that have arisen during the processing of your manuscript are listed below and are highlighted by flags in the proof. (AU indicates author queries; ED indicates editor queries; and TS/TY indicates typesetter queries.) Please check your proof carefully and answer all AU queries. Mark all corrections and query answers at the appropriate place in the proof using on-screen annotation in the PDF file. For a written tutorial on how to annotate PDFs, click http://www.elsevier.com/__data/assets/pdf_file/0007/98953/Annotating-PDFs-Adobe-Reader-9-X-or-XI.pdf. A video tutorial is also available at <http://www.screencast.com/t/9OIDFhigE9a>. Alternatively, you may compile them in a separate list and tick off below to indicate that you have answered the query.

Please return your input as instructed by the project manager.

Location in Chapter	Query / Remark
	There are no queries in this article <input data-bbox="1442 921 1497 970" type="checkbox"/>



CHAPTER ELEVEN

c0011 **Formation of Nanosized Products in Combustion of Metal Particles**

O.G. Glotov¹ and V.E. Zarko^{1,2}

¹Voevodsky Institute of Chemical Kinetics and Combustion, Siberian Branch of the Russian Academy of Sciences, Novosibirsk, Russia

²National Research Tomsk State University, Tomsk, Russia



s0010 **1. INTRODUCTION**

s0015 **1.1 Aluminum and Its Oxide Al₂O₃**

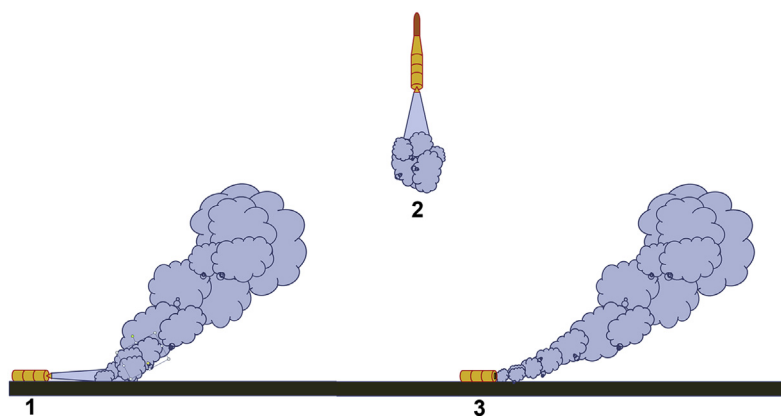
p0015 The idea of using metals of high caloric value (more than 2 kcal/g), such as beryllium, lithium, magnesium, aluminum (Al), zirconium, and titanium (Ti), as a fuel for rocket propellants was published independently and almost simultaneously by Russian scientists Yu. V. Kondratyuk (1929) and F. A. Tzander (1932) [1]. In the 1950s, the idea of metallized propellants was realized in practice by the Soviet Union (USSR) and the United States (US) and later on, by other countries. Among the metals mentioned, aluminum has been most widely used in solid propellants due to its high caloric value (≈ 9.8 kcal/g), comparative cheapness, and relative harmlessness of the main combustion product, oxide Al₂O₃.

p0020 Introducing aluminum into propellant formulation increases flame temperature and the velocity of combustion products, creating a jet thrust, improves the stability of motor operation by damping the gas oscillations in a combustion chamber, and makes it possible to control the propellant burning rate. At the same time, the presence of aluminum particles causes a great number of problems concerned with their behavior in combustion wave, combustion chamber, nozzle, and motor exhaust plume. Thus, a necessity arises to comprehensively investigate the ignition and combustion of Al particles in oxidizing media [1]. The efficiency of employing aluminum as a metal fuel is determined by the peculiarities of metal transformation into condensed combustion products. The transformation depends mainly on two processes: (1) the agglomeration of the primary particles of metal powder in a combustion wave, and (2) the burning of aluminum in the form of agglomerates or in the form of initial particles, followed by the formation of oxide particles. In the case of rocket motors, the above processes and subsequent evolution of oxide particles in the flow of gaseous combustion products determine the parameters of the size distribution function of oxide particles [2]. The size distribution functions of agglomerates and oxide particles and the data on the completeness of

aluminum combustion represent information that one needs to optimize propellant formulation and to estimate the different effects of the evolution of disperse phase (accumulation of slag in motors, nozzle erosion, two-phase losses of a specific impulse, damping of gas in combustion chamber). Outside the motor, the characteristics of oxide particles are of interest from two points of view: (1) the detection of rocket start from radiation of an exhaust jet, and (2) the ecological impact of rocket launching. Thus, the formation of aluminum oxide particles is not only of fundamental interest as a part of combustion mechanism but manifests a series of practical important aspects.

p0025 Let us discuss the ecological aspect. The life cycle of rocket engineering wares includes the designing, manufacturing, and testing of experimental items, the exploitation of stock-produced items, and their subsequent utilization either because of physical aging or for other reasons (e.g., the disposal of rockets according to international agreements on rocket elimination [3]), Figure 1. The actual ecological problems related to the above stages of the life cycle of rockets have been discussed in many reports, e.g., in Refs [4–15]. The well-known method of rocket disposal via open firing with a removed nozzle block is characterized by the following: (1) the localized release of a great amount of gaseous and solid combustion products and of concomitant substances, and (2) the burning of aluminum agglomerates at relatively low (as compared with the nominal one) pressure and also in the air at atmospheric pressure. These peculiarities give an impetus to the studies on the aerosol systems of oxide particles, especially within a nanosized range.

p0030 These particles are almost of no importance from the viewpoint of rocket motor performance but are of great essence for ecology. In particular, upon motor disposal, the concomitant substances, e.g., thermal protection materials, adhesive layer, etc., burn together with a propellant. Generally, combustion products contain toxic compounds,



f0010 **Figure 1** Combustion product emissions in the life cycle of a solid motor, one of the reasons for interest in the parameters of oxide nanoparticles: 1—testing; 2—exploration; 3—incineration (without nozzle).

e.g., dioxins [14]. Harmful substances may be located at the surface of alumina particles, in particular, of nanoparticles, which is favored by their high specific surface area. Therefore, laboratory studies are focused on the size distribution of particles, their concentration, and morphology. These characteristics determine the ability of particles to adsorb and transfer harmful substances in the atmosphere.

p0035 Thus, the interest in the characteristics of aluminum oxide nanoparticles is first motivated by the *ecological problems* of tests, exploitation, and utilization of rocket motors based on aluminized propellant. The second reason is related to the problems of *the technological combustion* of metallic fuel. In technological combustion, metal is used as a reagent for producing target products with given properties (oxides, nitrides, carbides, etc.) in various systems, i.e., pressed for self-propagating high-temperature synthesis (SHS), gelatinous (water gel) [16], loosed specimen, aerogel [17,18], aerodisperse [19–21], etc. It seems promising to employ the experience and results of the development of energy-releasing devices based on powdered fuel [19,20] to produce oxide nanoparticles with the given characteristics. In particular, the so-called method of gas-disperse synthesis of oxides has been developed [21]. It involves the burning of metal particles in a specially organized stationary, laminar two-phase flame. The method is characterized by the high purity of a target product (oxide), low manufacturing cost, high productivity, and ecological safety. In addition, the properties of the product may be controlled via variation of flame parameters. In particular, a considerable output of spherical nanoparticles of tens of nanometers can be achieved. Following, we will consider again the characteristics of oxide nanoparticles obtained by this method.

p0040 The problems of technological combustion of metal particles in the two-phase flame relate to the general problems of the mechanism of particle burning in a gaseous oxidizer. Knowing the laws of combustion, including the formation of oxide particles, may serve as the basis for understanding the mechanism of combustion and ensure the optimization of combustion process in technical devices.

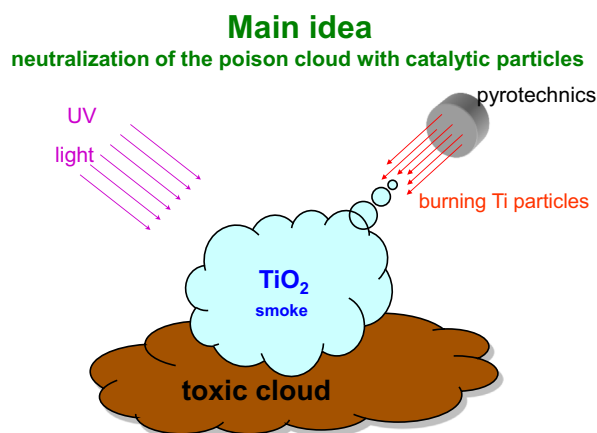
s0020 1.2 Titanium and Its Oxide TiO₂

p0045 Titanium, as aluminum, is the “aerospace” metal due to its lightness, strength, refractoriness, and corrosion resistance [22]. The fundamental investigations of Ti burning were carried out in the days of its introduction into technology as a structural material in the 1960–1970s. The goal of the studies was to determine the practical important characteristics (e.g., the burning rate depending on conditions) rather than to consider the combustion mechanism and formation of disperse combustion products. An alternative application of Ti powder as a metallic fuel (e.g., in pyrotechnical compositions, SHS systems, etc.) did not need either detailed understanding of combustion mechanism or information on oxide particles properties. In other words, as compared with Al, the needs of practical work did not stimulate studies on the mechanism of Ti combustion

in a gaseous oxidizer and no corresponding investigations were performed in the past. However, in 2005, it was proposed (probably first in Ref. [23]) to use the combustion of Ti particles in the air to form a cloud of photocatalytically active TiO_2 particles in order to deactivate either harmful or dangerous substances entering the atmosphere after an anthropogenic disaster or a terrorist act (Figure 2).

p0050 As a result, there was a revival of interest in Ti burning, confirmed by the appearance of experimental works in France, Germany, Russia, Ukraine, and the US. Studying the mechanism of Ti combustion appeared to be task oriented, i.e., aimed at solution of concrete problems. One of the tasks was to study the influence of burning conditions on the characteristics of resulting TiO_2 particles and to search for ways of controlling those characteristics. As in the case of technological Al burning, it was necessary to study the mechanism of particle combustion in order to develop the schemes of either process organization or technical device development, which provides an effective transformation of metal into oxide with the properties required. The researchers were interested in the size distribution of TiO_2 particles, their concentration (mass yield), and morphology. For Ti, an additional parameter of importance is the phase composition of TiO_2 particles. The latter is related to the photocatalytic activity of TiO_2 particles, which is usually determined in special experiments. Research on the technological combustion of Ti to obtain target products, in particular, oxide nanoparticles, is also underway [21].

p0055 Actually, the area of interest of the present work is limited by the combustion products of micron-sized aluminum and titanium particles. In the field of knowledge related to metallic fuels and their technical applications, micron particles are those that vary from units to hundreds of microns, whereas the particles of fractions of microns



f0015 **Figure 2** Idea to use a cloud of photocatalytic titanium dioxide nanoparticles to decontaminate atmospheric air, which inspired interest in studying the combustion of titanium microparticles in air.

(e.g., less than $0.1\ \mu\text{m}$) are commonly called the nanoparticles [24]. The object for analysis here are the nanosized oxide particles formed in combustion of the micron-sized Al and Ti particles. Let us also mention the following.

- o0010 1. There is a close relation between the examination of the *condensed combustion products* of metallized systems (composite aluminized solid propellants, pyrotechnical compositions with titanium, etc.) and the study of the process of *metal particles combustion* at the level of concepts, techniques, and even objects. On the one hand, the combustion of metallized compositions is characterized by the formation of the disperse phase, including agglomerates (the aggregated particles with a considerable portion of oxide, but containing active metal) and oxide particles with sizes from hundreds of microns to tens of nanometers. The disperse phase parameters of real compositions are necessary for engineering calculations and are measured in routine experiments. On the other hand, special metallized compositions may be used as a source of “mother” particles (i.e., burning particles that generate the oxide particles) in studies under various conditions (e.g., in a high-pressure vessel or in air at atmospheric pressure). This method may be used to produce particles that simulate agglomerates (i.e., comparatively large metal particles resulting from the combination of many small particles), formed in combustion of real composite systems. Thus, the preliminarily characterized “mother” particles of known dimensions, which burn in a specially produced gas medium, may serve as a physical model of the combustion of particle agglomerates in technical devices, e.g., in motor combustion chambers. As for experimental techniques, the essence of most of them reduces to the firing of particles in a vessel and to the sampling of combustion products for further analysis. Besides, one of the typical methods is the forced breaking of particle evolution (extinguishing of mother particles, freezing of oxide particles).
- o0015 2. The nanosized oxide particles present only one among many types of the condensed combustion products [2]. The nanoparticles may contribute just a minor fraction of all combustion products (on order of units of percent). However, they, as shown above, are of considerable interest but are poorly studied.
- o0020 3. The nanoparticles usually exist as aerosol systems and these systems are of considerable practical importance. Remember that the main parameters of nanoparticles, determined according to practical needs, are the size distribution of particles, their quantity (concentration, mass output), morphology (regularities of aggregation of primary particles, aggregate shape), and for TiO_2 , the phase composition (rutile/anatase/other phases).
- p0075 The chapter content is as follows. First, the techniques employed (mainly, the aerosol ones) are described. Then the experimental data on Al_2O_3 and TiO_2 nanoparticles, mainly the original data of the authors, are reported. In the conclusions, the actual problems are formulated and future investigations are discussed.

s0025

2. EXPERIMENTAL TECHNIQUES FOR PARTICLE SAMPLING

p0080

To analyze the disperse phase of burning metallized compositions (the combustion products of metallized particles), and to estimate the parameters of particle combustion macrokinetics, e.g., the combustion time, a series of original techniques have been developed at the Voevodsky Institute of Chemical Kinetics and Combustion, Siberian Branch of the Russian Academy of Sciences (ICKC SB RAS). Not all of the below methods were initially intended for studying nanoparticles. In most cases, the nanoparticles were sampled “among others,” i.e., together with larger particles. Particular attention has been paid to the capacity of different techniques to work within the given size range. In Refs [25] and [26], the entire arsenal of techniques was used to study the smoke combustion products of Ti particles. In Ref. [27], all the ICKC SB RAS techniques are presented as well as the main results obtained by these methods. Brief descriptions of them follow.

s0030 2.1 Flow-through Bomb for Sampling the Condensed Combustion Products of Metallized Compositions

p0085

The essence of sampling methods is to extinguish and to trap particles at various stages of combustion. Further study of sampled particles can be made by different available physical and chemical methods. This may provide a high informational content, and, at the same time, involve the development of corresponding analytical techniques and devices. In particular, for agglomerates and oxide particles, essential are the data on particle size, chemical, and phase composition. Different sampling methods for studying the condensed combustion products (CCPs) are employed in the US, Russia, Germany, Japan, Italy, Taiwan, and other countries. In 1985, at the ICKC SB RAS, an original technique was developed that exhibits a series of advantages as compared with other sampling methods. The various modifications of the technique have been repeatedly described in the Refs [2,25,28–34]. Briefly, a small propellant specimen is fired in a specially designed flow-through bomb pressurized with inert gas (N_2 , He, or Ar). The flame of the specimen is directed downward and enclosed in a “protective” tube, where the particles are in the gaseous combustion products of the specimen. Extinction is performed at the exit of the tube by mixing combustion products with a cocurrent flow of inert gas blowing through the bomb. The particles can be frozen at a given distance from the burning surface by varying the length of the protective tube. In the absence of the tube, the particles are extinguished at the shortest distance near the burning surface. Near the exit (inside the bomb), all the particles—combustion products generated by a propellant sample—are trapped by a wire mesh screen stack and by an analytical aerosol filter. The so-called “Petryanov” aerosol filter [35] (e.g., of AFA type) efficiently captures submicron particles. Briefly, the entrapping efficiency of AFA filters amounts to 95% for

the most penetrating particles—the standard oil aerosol with a diameter of 0.1–0.2 μm . Below we will consider the AFA filter characteristics and applications in more detail.

p0090 These are the real parameters at which the sampling of CCPs was performed: specimen diameter, 7–20 mm; length, 10–30 mm; and mass up to 5.5 g. When the diameter was 7 mm, the shortest distance of combustion products extinction was about 20 mm (ca. threefold specimen diameter). The maximal length of the protective tube was 190 mm. The maximal pressure was 12 MPa while the minimal one was 0.2 MPa. A low excess pressure is required for gas to flow through the bomb. In Ref. [25], the authors report experiments performed without a strong bomb casing, i.e., actually, at atmospheric pressure. The number of specimens, 1–5, in the series fired under the same conditions (tube length, pressure) depends on specimen size and is determined by the sampled mass needed for analysis. The optimum experimental conditions are provided by the presence of minimal mass, about 1.5 g of the particles sampled. Thus, for a typical metalized propellant, containing 15–25% Al, the total initial mass of specimens is about 5 g. The representativity of sampling, defined as the ratio between the calculated CCP mass and that of the CCP sampled, is not worse than 0.85; usually it equals 0.9–0.95 for aluminized propellants. In Ref. [34], a comparison has been made between the sampling representativity of the ICKC SB RAS technique and the technique of sampling into liquid for the combustion products of the propellant, containing Al-Mg mechanical alloy. In experiments performed at 0.3 and 6 MPa, the sampling representativity of the former technique was 0.57 and 0.80, and that of the latter was 0.27 and 0.61. Note that the Al-Mg alloy is a more “difficult” object than pure aluminum.

p0095 It is known that the combustion of metallized propellants results in the formation of particles differing in size by several orders of magnitude, e.g., from 10^{-10} to 10^{-2} m. The maximal size of the particles sampled by the ICKC SB RAS technique is unlimited. In particular, for some propellants we have sampled skeleton fragments of about 20 mm. The lower size limit for the particles analyzed is commonly equal to 0.5 μm . These are the data presented in our papers. However, it is due to the application of a granulometer “Malvern 3600E sizer” for analyzing small particles and is not a methodical limitation. As shown above, the AFA filter is effective in the trapping of nanometric particles. Figure 3(b) of Ref. [36] depicts the nanometric particles from the filter.

p0100 The mentioned extremely wide size range of CCP particles requires the application of special methods of particle size analysis to determine a size distribution function of particles. A typical method used by many researchers is either the physical or virtual (as a computational method) division of particles into fractions and the application of specific methods of analysis for each size range (fraction) followed by the computer combination of particular distribution functions and the recovery of a distribution function over the entire range. We have solved this problem using our algorithms and programs, described partly in Refs [28–30]. It is worth noting that the data on the chemical composition of particles (at least, in terms of the metal/oxide ratio) are

needed to evaluate the sampling representativity. The corresponding methods of analytical chemistry were developed and adapted [37–39] for a quantitative determination of both the metallic aluminum (called either active or unburned) content, and the “completeness of combustion” for dual metal fuels such as Al-B and Al-Mg. Obviously, the sampling method, as well as the other methods used to diagnose the disperse phase (e.g., photography/filming/video), face certain difficulties in interpreting the results obtained. For details, see Ref. [40].

s0035 2.2 Petryanov Filter

- p0105 The fibrous filtering materials, Petryanov filters (PFs), are serially manufactured and widely used in Russia [41]. The analytical aerosol Petryanov filter of AFA type was employed in Refs [26] and [27] as a tool for determining the total mass of smoke particles. In this case, a composite propellant specimen or a set of separate metallic particles were burned in a vessel of finite volume (10–20 L), and combustion products pumped through the filter during the time shorter than the sedimentation time of smoke particles in the vessel. If the particles were burned in air, the vessel was initially filled through the filter to prevent atmospheric aerosol from penetration into the vessel.
- p0110 According to Ref. [35], for the AFA filters, the trapping efficiency, E , determined using a standard oil aerosol, is about 95% for the particles with a diameter of 0.1–0.2 μm . The particles of this size are most penetrating. For other sizes, the efficiency is higher, namely, $E \geq 99\%$, for those with a diameter of 0.3 μm ; $E \geq 99.99\%$, for the particles of 1 μm ; $E \geq 99\%$, for the particles smaller than 0.1 μm ; and $E \geq 99.9\%$ for those of 0.02–0.05 μm . In addition to the high efficiency of particle trapping due to electrostatic charge, the particles can be easily removed from the filters by dissolving the AFA filter in acetone. The resulting suspension of particles can be analyzed using, e.g., an automatic granulometer “Malvern 3600E.” The procedure for making the filter optically transparent via impregnation with glycerine is described in Ref. [36]. Thereafter, the particles of tens of microns can be examined and measured under an optical microscope without removing them from the filter.
- p0115 The Petryanov filters, made of perchlorvinyl fibers, are hydrophobic (the maximal relative humidity of filtered air being 95%), chemically resistant relative to liquid aerosol particles of mineral acids and alkali, but of low thermal resistance (up to 60 °C) and are unstable to oils and organic solvents of the type of plasticators, chlorinated hydrocarbons, etc. The Petryanov filters made of acetylcellulose fibers are hydrophilic and chemically stable to organic solvents of the type of plasticators and oils, but are unstable to acids, alkali, and organic solvents, such as dichloroethane, acetone, etc. Their thermal resistance is limited to 150 °C, the maximal relative humidity of filtered air is 80%. Thus, the main disadvantages of the both types of the Petryanov filters are the limited thermal resistance and the stability to chemically active materials as well as the low filtration rate (about 1 cm/s).

- p0120 We have tried to estimate the specific surface of filter fibers by the “Sorbi” apparatus, using the BET method. The idea was to measure filter surface prior to experiments and then to sample particles and to measure the surface once again. In this case, the difference in surface values before and after experiment with account for the mass of the particles sampled would provide the specific surface of the particles sampled. Our efforts have failed because it was impossible to correctly measure the filter surface which varied continuously, probably, due to the destruction of filter fibers at cryogenic temperature at which the working gas is adsorbed by the Brunauer–Emmett–Teller (BET) method.
- p0125 The advantages and disadvantages of the Petryanov filter are presented in detail in Ref. [41].

s0040 2.3 Aerosol Impactor

- p0130 A cascade impactor of Anderson type [42] was employed together with the Petryanov filters [26,27]. The impactor is used to perform the aerodynamic size classification of particles. Each cascade consists of two plates: the first one is with apertures and the second is used to sample particles. The flow of particles moves to the surface of a sampling plate. The cascades differ in diameter, the number of apertures, and the distance between the plates. They are characterized by the size of particles, deposited on a plate at a certain airflow rate. We have used a five-cascade impactor “BP-35/25-4,” elaborated and manufactured at the state scientific center of virology and biotechnology “Vector” (Novosibirsk region, Koltsovo). The nominal, characteristic size of particles, d_{50} , trapped by cascade #1 is 17.8 μm , 13.5 μm for cascade #2, 3.65 μm for cascade #3 and 1.27 μm for cascade #4 (calculations were performed for particles of a density of 3.9 g/cm^3). The AFA filter that traps the particles passing through cascades 1 \div 4, plays a role of the fifth cascade. This impactor allows one to estimate the mass size distribution of smoke particles, including the fraction of those smaller than 1.27 μm . As in the case of the filter, a vacuum pump and a device to control a gas flow rate are needed for the impactor to work.

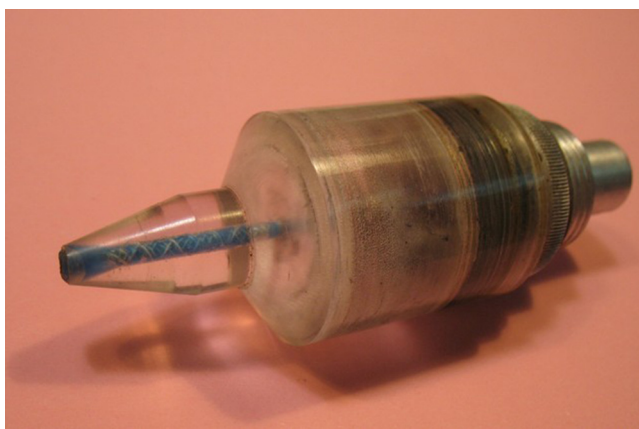
s0045 2.4 Diffusion Aerosol Spectrometer

- p0135 The diffusion aerosol spectrometer (DSA), developed at the ICKC SB RAS [43], includes diffusion battery, condensation enlarger, and optical counter of particles. It is used to determine the size and concentration of aerosol particles. Such measurements are regulated by a state standard [44], where the working principle of the setup is presented. For description and a block scheme, see Ref. [43]. The basic technical characteristics of the DSA are as follows. The measured particle diameters are 3 nm \div 1 μm , the concentration range of aerosol particles is $10^1 \div 5 \times 10^5 \text{ cm}^{-3}$, and the measuring cycle lasts 5 min. By the given characteristics, the DSA is either in line with the best foreign aerosol spectrometers [45,46] or even better.

p0140 The DSA was employed to study the nanosized oxide smoke TiO_2 aerosol, formed by combustion of tiny specimens of pyrotechnic composition with titanium powder [25]. It was shown that the mean arithmetic size of particles, D_{10} , determined by the DSA, coincides well with that obtained by a laborious detailed treatment of electron-microscopic images (the particles with $D_{10} \sim 20$ nm). Thus, the DSA can be recommended for studying the aerosols of nanoparticles resulting from the combustion of metal particles.

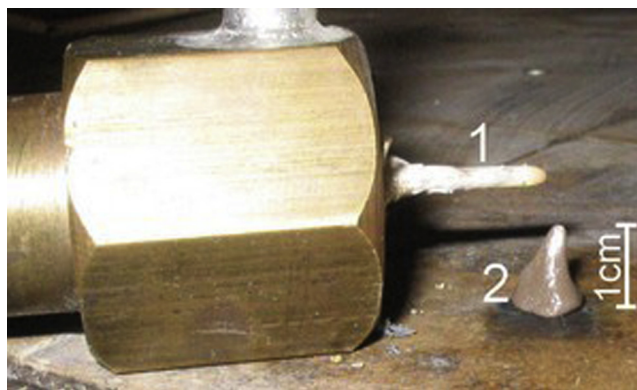
s0050 2.5 Vacuum Sampler

p0145 A vacuum sampler is a device, similar by its sampling principle, to the probe of molecular-beam mass spectrometry, applied for studying the flame structure of condensed systems [47], and by its deposition principle, to a low-pressure cascade impactor [42]. The vacuum sampler for trapping submicron particles from specimen flame or from vessel volume is of the form of a steel capillary tube. One of its ends is located in the flow of the two-phase medium studied, and the other is in the vacuumized volume that contains a screen with Formvar film that serves as a substrate for inertially deposited particles. This system, screen + film + particles, is the commonly used object for a transmission electron microscope. Other substrates are also possible, e.g., the silicon ones for a scanning electron microscope. The sampler parameters (capillary diameter, the degree of rarefaction, the distance between tube end and a substrate) are to be chosen with regard to the given particle size range. Available are a variant for “cold” aerosols with a conic, Plexiglas tip (Figure 3), and that with a ceramic capillary for sampling from flame (Figure 4). The sampler is calibrated using standard aerosols. The residence time of particles in a working volume of the sampler (from their takeout from flame to deposition on a substrate) varies, depending on sampler parameters, from 1 to 100 ms. In Ref. [25], we have used the vacuum sampler, developed and patented by the researchers



f0020

Figure 3 Vacuum sampler—a variant for cold flows with Plexiglas tip (to the left).

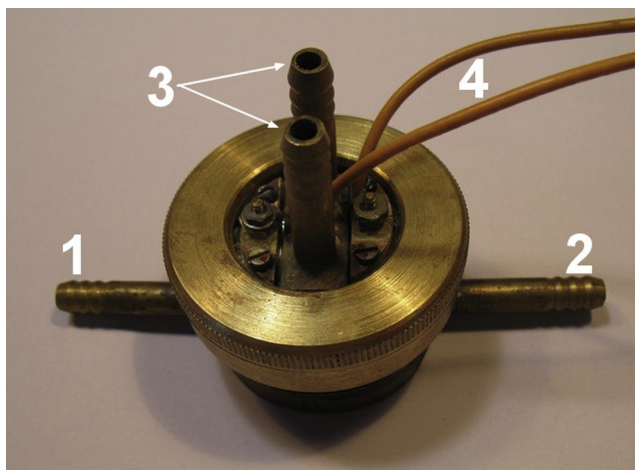


f0025 **Figure 4** Vacuum sampler—a variant for aerosol sampling from flame. 1—capillary, 2—specimen of pyrotechnical composition.

of the ICKC SB RAS [48,49]. Experiments were performed as follows. A conic specimen of titanium-containing pyrotechnical composition of a height of 1 cm was fired in air at atmospheric pressure. Aerosols were sampled upon combustion from flame through a ceramic capillary 3 cm long with 1 mm inner diameter under relatively small rarefaction (pressure drop of a 20 mm water lift relative to atmospheric pressure) (Figure 4). The aerosol sampled was diluted with purified air at a flow rate of 10 L/min and sent to a 20-L buffer vessel from which it was directed to the diffusion aerosol spectrometer, DSA. It is assumed then that a fast dilution allows us to avoid the formation of aerosol aggregates. A typical aerosol concentration in the buffer vessel was 10^4 – 10^5 cm^{-3} . In the previous section, it was recommended to use the DSA for studying the aerosols of nanoparticles, formed in combustion of metal particles. This section demonstrates the application of a vacuum sampler for collecting aerosol particles from flame. In this case, the following considerations should be taken into account. If aerosol particles are of complex structure, e.g., in the form of fractal aggregates consisting of primary nanoparticles, it is likely that these aggregates will be destroyed upon sampling and transportation through a capillary under the action of aerodynamic forces. In other words, information on aggregate structure will be lost upon sampling. If a researcher is interested only in the parameters of the primary particles, the use of the vacuum sampler together with the DSA is a good combination. However, when the researcher takes so much interest in aggregate structure (as shown in the introduction, it plays a key role upon aerosol propagation in the atmosphere), then he should use more “delicate” methods of sampling, e.g., a thermophoretic precipitator that is described below.

s0055 2.6 Thermophoretic Precipitator

p0150 In all our works, the data on the morphology of oxide aerosols were extracted from particle sampling with a thermophoretic precipitator, developed and produced at the



f0030 **Figure 5** Thermophoretic precipitator. 1,2—inlet and outlet water sockets for cooling the lower wall of the channel; 3—inlet and outlet aerosol sockets; 4—wires for electric heating of the upper wall of the channel.

ICKC SB RAS. The setup is shown in [Figure 5](#); for details see Ref. [\[50\]](#). The apparatus provides a nonselective sampling of particles with an efficiency close to 100% over a size range of 3 nm–10 μm on the screen with Formvar film, used for subsequent examination under transmission electron microscope. The principle of operation is the following. There is a channel of rectangular cross-section 5 mm wide and 100 μm high. The temperature gradients of 2200–2400 K/cm were set by heating the upper wall of the channel with electric current and by cooling the bottom wall with running water. The walls of the channel are made of bronze. The set of screens with Formvar film are fixed on the lower wall. Aerosol moves slowly through the channel (mass flow rate being below 15 sccm—standard cubic centimeter per minute). The molecules of carrier gas, which move more vigorously near the heated plate, gradually push away the aerosol particles toward the cold plate until their deposition on the screen. After the experiment, the screens are removed and studied by electron microscope. The electron-microscopic images are treated using original software [\[28–30,51\]](#).

s0060

3. ORIGINAL EXPERIMENTAL APPROACHES

s0065

3.1 Preparation of Monodisperse Agglomerate Particles

p0155 The development of special laboratory technologies for producing the burning monodisperse particles of agglomerate origin (i.e., resulting from joining many small particles) has two main motives.

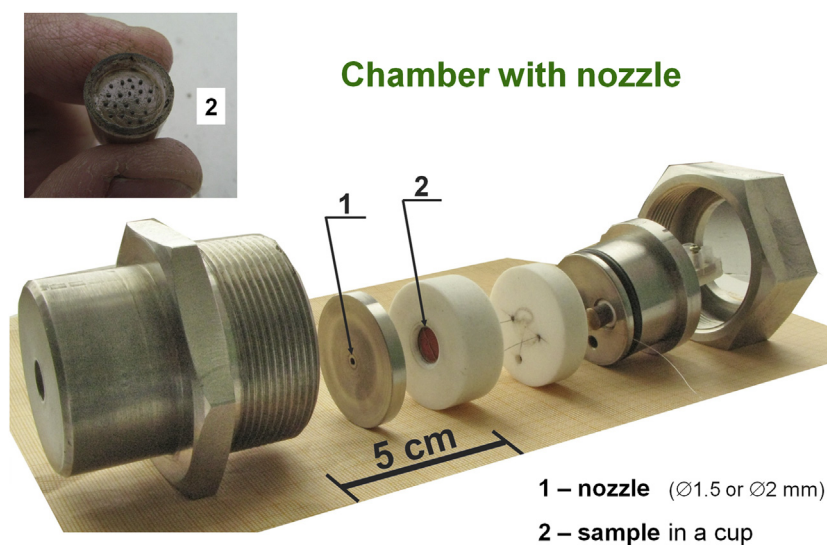
- p0160 First, the identical particles are the most convenient objects for studying combustion mechanism in general and oxide particle formation, in particular. Particle polydispersity causes the well-known difficulties in interpreting sampling results [40]. The particles of various sizes exhibit different behaviors in gas flows. They are characterized by individual temporal parameters, e.g., the time required to cover distance up to extinction in extinguishing and sampling techniques. Moreover, the macrokinetics of the combustion of various sized particles is different ~~for~~ the general case, probably due to distinctions in the structure and morphology of particles, in particular, due to the metal/oxide ratio. Thus, performing experiments on the particles of a given size and of the same structure provides the most accurate and reliable data.
- p0165 Second, in most of the cases (except for technological particle combustion in a dust jet, see the introduction), researchers deal with the combustion of agglomerates rather than of single monolithic particles. The regularities of agglomerate combustion should be examined because of their practical importance. In the general case, the combustion of solid particles and agglomerates is different. For example, the formation of burning 500 μm aluminum agglomerates in combustion of composite solid propellants is a common practice [52]. At the same time, a 500 μm solid aluminum particle can be ignited only when using a powerful CO_2 laser. Therefore, the relevance of the application of a solid particle as a physical model of an agglomerate needs to be proved. For aluminum particles, it can be assumed that the smaller the particle or the agglomerate, the smaller are the distinctions in their combustion parameters (the time of complete combustion, i.e., burning time; a fraction of formed highly disperse oxide, etc.). To orient someone, remember a diameter value of 100 μm . It is shown [54] that the combustion behavior of agglomerates and particles of this diameter is almost the same. Similar information is unavailable for titanium particles.
- p0170 We have developed an original approach to produce monodisperse burning agglomerates of aluminum and titanium just during experiment. The details of its realization for aluminum and titanium are different, but, in both of the cases, the approach is based on the transformation of dosed microquantities of highly metallized composition into individual burning particles. The transformation is performed in a combustion wave of nonmetallized composition in which the above microquantities of metallized composition are contained as inclusions. The mass, size, and composition of inclusions determine the parameters of burning particle agglomerates. The main experimental difficulty in realizing this approach is that the inclusions should be identical. Nevertheless, we have managed to produce the particles with a variation coefficient K_{var} in the range $0.07 \div 0.14$. Notice, that in granulometry, the set of particles with variation coefficients $K_{\text{var}} < 0.15$ ([53], p. 212), is assumed to be monodisperse. Here $K_{\text{var}} = \sigma/D_{10}$, and $\sigma = \sqrt{D_{20}^2 - D_{10}^2}$ is the mean-square deviation (standard deviation).

p0175 Using this approach, we have already produced and studied the burning agglomerates of aluminum 100, 340, and 480 μm in diameter, and those of titanium 300, 390, and 480 μm in diameter. The technology of producing inclusions and specimens as well as the results are fully presented in Refs [36,40,54,55–57] for aluminum agglomerates and in Refs [58–64] for the titanium ones.

s0070 3.2 Chamber with Nozzle for Particle Acceleration

p0180 Analyzing the literature and our own data on titanium particle combustion, we assumed that the combustion parameters (including the characteristics of nanosized oxide) depend on the velocity of burning particles in a gaseous oxidizing medium [26]. To verify this assumption, we have constructed a setup in the form of a small chamber with a nozzle (Figure 6).

p0185 In the chamber, a specimen burns to generate monodisperse burning particles, which are ejected through the nozzle. Firstly, the particles are transported mainly by a jet of gaseous combustion products. Then, the jet is decelerated and dissipated in the ambient air, and the particles move under their own momentum, the Stokes drag force, and the gravity force. The regularities of particle movement in each case (particle diameter, nozzle diameter, up/down direction, etc.) should be studied in detail and generalized statistically for a set of particles of the given nominal size. Note that the influence on the combustion process is related not to the absolute value of particle velocity but to the velocity of movement relative to the ambient air, i.e., the relative flow velocity [63,64].



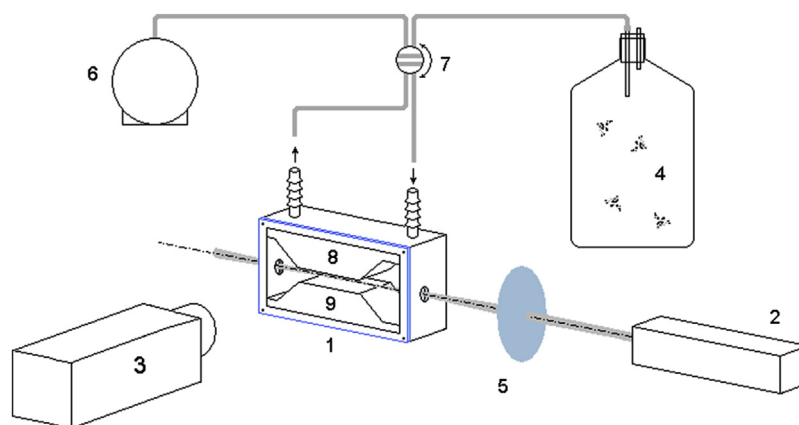
f0035 **Figure 6** Knocked-down chamber with nozzle. At the top left, there is a specimen of “nonmetalized matrix + metalized inclusions” type upon preparation. The preparation involves a gradual filling of a small cup by successive formation of matrix and particle layers.

In this case, the smaller particles acquire the velocity of either the jet or the ambient gas more quickly so that a blow velocity becomes zero. When the nozzle is 1.5 mm (the minimal value in our experiments) for particles with a diameter of $320\ \mu\text{m}$, a relative blow velocity, averaged along the entire trajectory, reaches 7.9 m/s. To increase the mean blow velocity one should solve the optimization problem, taking into account the parameters that determine particle motion and burning. The main parameters are: burning rate, temperature, specimen geometry, nozzle diameter, determining the outlet jet characteristics, the diameter and aerodynamic drag force coefficient of burning particles that determine particle acceleration/deceleration ratio, and burning time. The last one determines the time range for averaging. Usually, the motion of particles is recorded using a video camera. Thus, in Refs [63] and [64], the shooting was performed at the rate of 300 fps.

s0075 3.3 Video Microscopy in Aerosol Optical Cell of Millikan Type

p0190 The setup is schematically depicted in Figure 7 (taken from Ref. [65] by authority of the author of the method). The optically accessible aerosol cell (similar to those of Millikan, Fuchs, Petryanov) has two windows for a laser beam to pass and one window to record particle images, resulting from light scattering at an angle of 90° , with the help of a video camera. The visualized field is located between metallic, parallel electrodes to which a voltage is supplied. The pump is used to inject an aerosol sample into the cell. The valve is then turned off and the behavior of the aerosol sample is recorded.

p0195 Specifications of the setup are as follows. The power of helium–neon laser amounts to 2.5 mW. Focusing optical instruments allow one to get an effective beam diameter in a bottleneck within the range $150\text{--}350\ \mu\text{m}$. The gap between the electrodes is 2.5 mm;



f0040 **Figure 7** Block-scheme of the system of videomicroscope and aerosol cell [65]: 1—cell; 2—laser; 3—CCD camera with microscope lens; 4—vessel in which the samples, generating aerosol, were burned; 5—lens; 6—pump; 7—double valve; 8,9—electrodes in the cell.

the strength of homogeneous electric field is 160–360 V/cm. A black-and-white camera with a microscope lens provides observation of the working volume region of the cell with $\approx 15\times$ magnification on the camera charged-coupled device (CCD) matrix. The spatial resolution of the system (lens + CCD matrix) is about 3 μm , the focal depth is about 50 μm , and the visualized field of vision in the working volume of the cell is about $300 \times 400 \mu\text{m}^2$. The lower limit to the size of the particles recorded amounts to about 0.1 μm and is limited to the sensitivity of the CCD matrix and the density of laser radiation flux in the volume visualized. The particles smaller than 3 μm are observed as light spots, which makes it possible to follow their movement. The shape of the particles exceeding 3 μm in size can be distinguished, which allows one to observe their rotational motion (e.g., under the action of electric field).

p0200 Thus, this technique may be used to follow the motion of aerosol particles with or without electric field and to determine the velocities of photophoresis and Brownian motion, the electric charge, and charge-dipole moment, and the other parameters of single aerosol particles using an ultra-low mass aerosol sample (ten-hundreds of picograms, tens of particles).

s0080



4. CHARACTERISTICS OF OXIDE NANOPARTICLES

s0085

4.1 Aluminum Oxide Al_2O_3

p0205 The literature data on aluminum oxide nanoparticles, formed in combustion of aluminum microparticles, are rather scarce. The method of gas-disperse synthesis of metal oxide nanopowders in a laminar aerodisperse flame was developed at the Odessa National University (Ukraine). It was referenced in the introduction as an example of technological combustion. For technological purposes, the laminar flame is usually used. In this case, the reaction zone is narrow, of almost permanent thickness over the flame surface, with high temperature gradients in preflame and postflame zones, and without recirculation of combustion products. As a result, metal burning and the condensation of combustion products occur along the entire height of the flame zone (conically shaped) almost under the same conditions. The influence of particle coagulation on the size distribution of combustion products is negligible, which favors the production of the narrow fractions of combustion products. The attempt to increase the output of the setup at the expense of turbulization leads to the polydispersity of condensed combustion products.

p0210 Reference [21] summarizes the main results of experimental and theoretical studies on the effect of the parameters of the aerodisperse diffusion flame of metal particles (Al, Fe, Ti, Zr) on the dispersity of the combustion products of these metals in oxygen-containing media. The authors [21] have varied the mass concentrations of fuel and oxidizer, the nature of carrier gas, and the method for flame organizing: laminar diffusion flame (LDF) or premixed laminar flame (PLF). These results [21] are presented in Tables 1 and 2.

t0015 **Table 1** The parameters of aluminum oxide particle size distribution. Effect of initial oxygen concentration C_{O_2} . Initial aluminum particles: mass concentration $C_f = 0.4 \text{ kg/m}^3$, size $d_{10}^{Al} = 4.8 \text{ }\mu\text{m}$.

$C_{O_2}, \%$	Carrier gas	$d_{10}, \text{ nm}$	$d_{20}, \text{ nm}$	$d_{30}, \text{ nm}$	$D_x, \text{ nm}$	σ	$d_{50}, \text{ nm}$	$d_m, \text{ nm}$	$S_c, 10^4 \text{ m}^2/\text{kg}$
0	N ₂	103	126	150	73	0.62	77	62	2.4
6.4		83	94	104	44	0.47	75	64	2.3
11.6		69	76	83	32	0.38	66	60	2.7
14.0		61	65	70	22	0.53	58	54	2.8
27.0	He	63	69	78	28	0.35	59	55	2.7
20.0		53	57	60	21	0.31	52	51	3.1

t0020 **Table 2** The parameters of aluminum oxide particle size distribution obtained in premixed laminar flame (PLF) regime. Effect of initial aluminum size d_{10}^{Al} and concentration C_f .

$C_f, \text{ kg/m}^3$	$d_{10}^{Al}, \text{ micron}$	$d_{10}, \text{ nm}$	$d_{20}, \text{ nm}$	$d_{30}, \text{ nm}$	$D_x, \text{ nm}$	σ	$d_{50}, \text{ nm}$	$d_m, \text{ nm}$	$S_c, 10^4 \text{ m}^2/\text{kg}$
0.22	4.8	83	100	119	56	0.57	66	51	2.7
0.40		103	126	150	73	0.62	77	62	2.1
0.62		107	127	152	68	0.63	91	69	1.9
0.7	14.6	71	81	92	39	0.50	63	49	2.7

p0215 The parameters used in Tables 1 and 2 are denoted as follows: C_f and C_{O_2} are the mass concentrations of metal fuel and oxygen in the carrier gas, and d_{10} , d_{20} , d_{30} are the arithmetic mean, surface mean, and volumetric mean diameters, correspondingly. These diameters are determined by the formula $d_{mn} = \sqrt[m-n]{(\sum_{i=1}^k d_i^m \cdot N_i) / (\sum_{i=1}^k d_i^n \cdot N_i)}$, where m , and n are the integers setting the order of the mean diameter, k is the total number of size intervals in histogram, N_i is the number of particles in the i -th interval, and d_i is the middle of the i -th interval. The parameter D_x is the standard deviation determined by the formula $D_x = \sqrt{d_{20}^2 - d_{10}^2}$, σ and d_{50} are the parameters of the lognormal distribution function of oxide particles in the form $\phi(d) = \frac{1}{\sqrt{2\pi} d \sigma} \exp\left[-\frac{(\ln d - \ln d_{50})^2}{2\sigma^2}\right]$. For the distribution formula of this type, the parameter σ is called “width” and the parameter d_{50} is called “median.” These parameters may be used to calculate “mode” d_m , “specific surface” S_c , and other useful parameters. For instance, $d_m = d_{50} \exp(-\sigma^2)$, $S_c = 6/(\rho d_{32})$, where ρ is the oxide particles density, and $d_{32} = (d_{30})^3 / (d_{20})^2$. The mean diameters d_{20} and d_{30} can be calculated using the lognormal size distribution parameter from the common formula $(d_r)_r = (d_{50})^r \exp(r^2 \sigma^2 / 2)$, where r is the integer.

p0220 As follows from Tables 1 and 2, the mean diameter d_{10} varies from 53 to 103 nm. The position of a maximum of the lognormal distribution of oxide particles, mode d_m , varies slightly ($d_m = 49-69 \text{ nm}$) within the experimental conditions range studied by

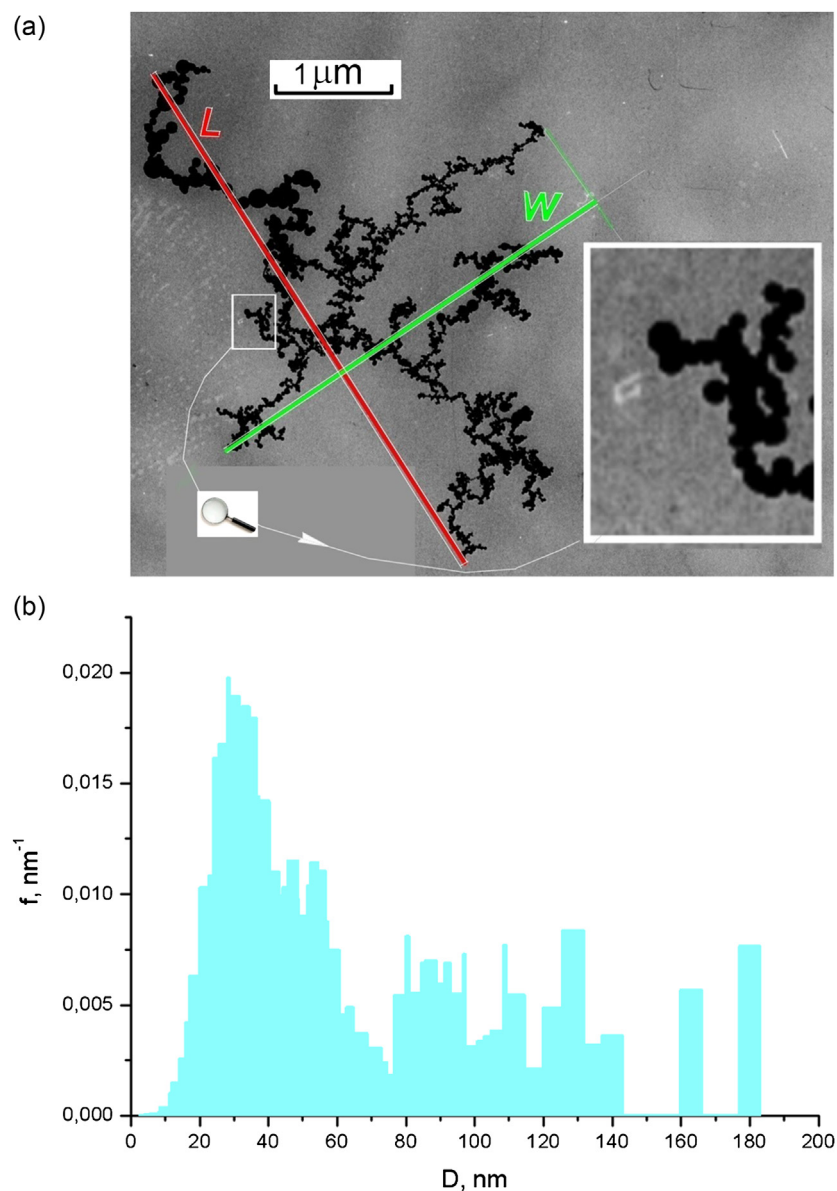
the authors [21]. The influence of experimental conditions on the dispersity of Al combustion products reduces mainly to the variation of the width σ of the particle size distribution function ($0.31 < \sigma < 0.63$).

p0225 To control the dispersity of oxide nanoparticles, the authors [21] suggested introducing admixtures into the primary metallic fuel to affect oxide nucleation in flame via ionization. The ions are assumed to be the centers of condensation. Increasing their concentration leads to an increase in combustion products dispersion. This assumption was verified experimentally [21]. Thus, adding 5% carbon (mechanical mixture of 95% Al and 5% C) causes the decrease in d_{10} from 103 nm to 34 nm and in d_m from 62 nm to 30 nm.

p0230 As compared with Ref. [21], in our works [57,65–67,69–75], the oxide particles were characterized by several techniques. When performing “delicate” sampling of aerosol particles with a thermophoretic precipitator followed by the analysis of samples by means of transmission electron microscope (TEM), we have managed to study not only the distribution functions of the primary nanoparticles but also the aggregates, consisting of nanoparticles, to obtain information on their morphology, phase composition, etc. The video microscopy made it possible to investigate the charge (and dipole) properties of the aggregates, their mobility, coagulation, and other characteristics. As mentioned in the introduction, the morphology of aggregates determines their transport properties (diffusion coefficient, sedimentation and velocity of photophoresis, etc.), optical characteristics, specific surface, and the ability to adsorb and transfer harmful substances. As is known, the charge properties of nanoparticles and of their aggregates have a substantial effect on aggregate formation and evolution. The typical features of evolution are the change in size due to the merging of the aggregates and single particles (coagulation) owing to the Coulomb interaction, and the restructuring (swerving) of the aggregates.

p0235 Consider now the main results from experiments [67] on the combustion of model aluminized composite propellant, containing 20% Al, 25% AP, 35% HMX, and 20% binder (the same as in Ref. [57]). The specimens in the form of a parallelepiped 20–25 mm long and with a cross-section of $1 \times 1.5 \text{ mm}^2$ were burned in a ~~20-l~~ vessel in the aerosol-free air at atmospheric pressure. The aluminum mass of the specimen was ≈ 6 mg. The burning surface generated aluminum agglomerates with a wide size distribution. They burned upon their fall in the vessel for less than 5 s. Six minutes after propellant burning, the aerosol was sampled from the vessel and its disperse, morphological, and charge characteristics were analyzed. The time value of 6 min can be called the “age” of the aggregates.

p0240 Figure 8 shows a typical TEM image of the aluminum oxide aggregate. As follows, the aggregate is chain branched and consists of the primary spherical particles from units to hundreds of nanometers. These particles are called *spherules*. The images were processed to determine the conventional aggregate size R , the number of spherules, and



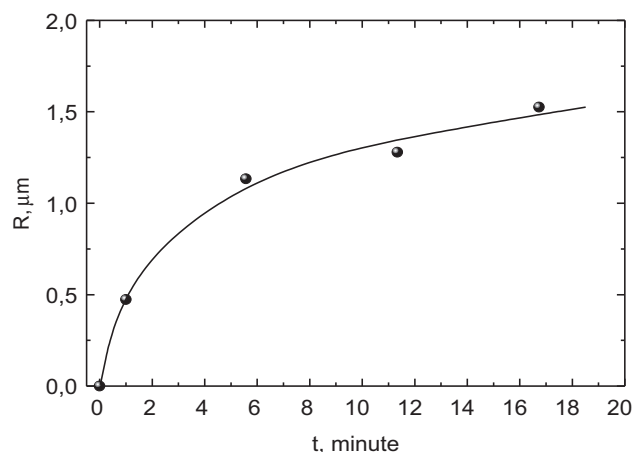
f0045 **Figure 8** (a) A typical view of aluminum oxide aggregate. (b) Mass size distribution function for spherules of which this aggregate is composed.

their size distribution, see [Figure 8](#). Taking into account particle density, on the basis of these data one can readily calculate the aggregate mass M . The structural characteristics of similar aggregates are usually characterized in terms of the fractal dimension D_f . According to Ref. [68], D_f may be defined as an exponent in the power relationship

$M \propto R^{D_f}$ between the aggregate mass M and its size R . Actually, this approach is based on the assumption of a minor “overlap” of spherules in the image, so that the aggregate projection onto the plane corresponds to the volumetric distribution of spherules in the aggregate. If $D_f < 2$, the fractal dimension of two-dimensional projection is equivalent to that of the three-dimensional object [76]. In Ref. [67], the fractal dimension D_f was found for a set of aggregates, “on average.” In this case, a mathematical procedure reduces to the determination of the slope of the straight line, which approximates the size dependency of the mass in logarithmic coordinates $\log(M)$ versus $\log(R)$. Note that there are the alternative ways of estimating the fractal dimension and the size of aggregates. Some of these are discussed in Ref. [51]. In Ref. [67], the authors plotted $\log(M)$ versus $\log(R)$ and got $D_f = 1.60 \pm 0.04$. A total of 52 aggregates at age of 6 min were processed. The convention size R varies from 0.09 to 2.31 μm , and the number of spherules varies from 20 to 3280.

p0245 In Figure 8, the fragment in the white frame and its enlarged image demonstrate that the aggregate consists of spherules. It is worth noting that the aggregate contains “clusters,” i.e., the regions with particles of visibly different size range. This aggregate was treated using three different magnifications for the different parts of the aggregate. The aggregate includes totally 3217 spherules. Plot (b) presents the mass size distribution function $f(D)$ of aggregate spherules. The value f , a relative spherule mass within the histogram size interval, divided by interval width, is plotted on the ordinate. Figure 8(a) illustrates one of the ways to determine a conventional aggregate size or “radius” from the expression $R = 0.5\sqrt{LW}$, where L is the maximal length, and W is the width, the maximal aggregate size in the direction perpendicular to L . For this aggregate, we get $L = 4.96 \mu\text{m}$, $W = 3.79 \mu\text{m}$, and $R = 2.17 \mu\text{m}$. For comparison: the nominal radius of the sphere with a volume equal to the total one of spherules in the aggregate is 0.256 μm .

p0250 For the above-mentioned model propellant, there are different statistics [57], supplemented with the data on 18 aggregates at an age of 12 min. In this case, we have $D_f = 1.64 \pm 0.09$. Besides, in Ref. [57], another technique has been used to estimate the conventional aggregate size. Nevertheless, the derived values of fractal dimension $D_f = 1.60 \pm 0.04$ and $D_f = 1.64 \pm 0.09$ coincide to within experimental error and are noticeably lower than 1.80, which corresponds to the DLCCA model (diffusion-limited cluster–cluster aggregation) [76]. For this model it is assumed that the aggregates merge exclusively due to the Brownian diffusion without long-range interactions between them. As shown below, the process of coagulation of the aerosol particles under study involves electrostatic forces, i.e., those of the Coulomb interaction, determined by the presence of electric charges. Distributed charges promote the formation of “chain” fragments (clusters) in the aggregate structure. The greater the number of such fragments in the aggregate, the closer to 1 is D_f (for a linear chain of spherules $M \propto R$). We may say that the value of D_f deviation from 1.80 characterizes the role and significance of the Coulomb interaction in aggregate formation and evolution.



f0050

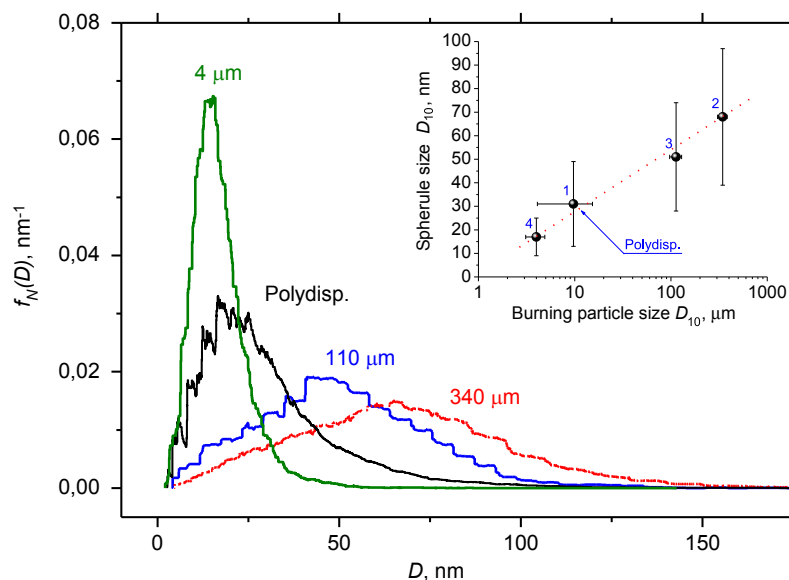
Figure 9 Arithmetic mean radius of aggregates versus coagulation time.

p0255 The dependency of aggregate size on age (coagulation time) was revealed in Ref. [69] (Figure 9). The observed asymptotic character of the dependency, is, probably, determined by a limited number of aggregates in a vessel. The greater the number of the aggregates that have already merged, the less is the probability of the subsequent collisions.

p0260 The presence of clusters, in which the difference in spherule size is rather small, but at the same time, the difference in spherule size from cluster to cluster is essential (Figure 8), may be explained as follows. The clusters with spherules within a certain comparatively narrow range were first formed by various mother particles. Then these merged into an aggregate via coagulation. This assumption is based on the hypothesis that the size of spherules depends on the size of a burning original particle. The hypothesis was later verified by experiments on monodisperse burning particles [57]. Indeed, the greater the diameter of the mother particle, the larger are the spherules formed, see Figure 10 and Table 3.

p0265 Figure 10 shows the joint functions of the normalized density of the size distribution of a number of spherules obtained by combining histograms for the set of aggregates. Numbers near the curves denote the diameter of burning particles. The curve “Polydisp.” corresponds to the population of particles-agglomerates, generated by combustion of composite propellants. In this case, the efficient diameter of the burning particles is estimated as $\approx 10 \mu\text{m}$, which corresponds to the mean arithmetic diameter of aluminum particles used to manufacture the propellant. The insert plots the arithmetic mean spherule diameter versus that of the burning particles.

p0270 The data in Figure 10 and Table 3 indicate that the spherules, formed by combustion of a polydisperse system, exhibit a wider size distribution ($K_{\text{var}} = 0.58$, whereas for



f0055 **Figure 10** Effect of the size of burning particles on the size distribution of formed oxide nanoparticles. Here, 4 μm , 110 μm , 340 μm and “Polydisp.” are the sizes of burning particles.

t0025 **Table 3** Dependency of the parameters of oxide spherules dispersity on the size of burning particles [57].

Point no. in Figure 10 insert	Size of burning particle, micron	Number of treated spherules	D_{10} , nm	D_{20} , nm	D_{30} , nm	D_{43} , nm	σ , nm	K_{var}
1	Polydisperse	44,843	31	36	43	80	18	0.58
2	340	14,348	68	74	80	107	29	0.43
3	110	14,296	51	56	61	80	23	0.45
4	4	48,885	17	19	21	34	8	0.50

monodisperse particles, $K_{\text{var}} = 0.43\text{--}0.50$). According to the results of determining the fractal dimension of the aggregates, the values of D_f vary from 1.62 to 1.65 in the case of 10–340 μm burning particles. For the burning particles of 4 μm , $D_f = 1.80$, which corresponds to the DLCCA model and indicates the reduced role of the Coulomb interaction as compared to the Brownian diffusion with decreasing sizes of spherules and/or burning particles. It is interesting that the value of the fractal dimension is actually independent of coagulation time within the range studied (up to 17 min).

p0275 Our data (Table 3) on the sizes of Al_2O_3 spherules and those of Ref. [21] (Tables 1 and 2) are mutually complementary. In particular, our data were used in Ref. [21] to construct the dependency of spherule size on the mass concentration of metals (see Figure 6 in Ref. [21]).

- p0280 Video microscopy makes it possible to observe a series of phenomena to be interpreted quite plainly.
- o0025 1. The movement of charged (negative or positive) aggregates in a homogeneous electric field of 160 V/cm. The motion direction changes with changing field polarity. A minor part of aggregates does not respond to field switching. Thus, many aggregates carry an electric charge, which can be either positive or negative.
- o0030 2. The rotation of some aggregates by 180 degree when switching the electric field polarity. Interpretation: such aggregates have a distributed electric charge and a rotating moment appears in the electric field. The (+) and (-) charges may be compensated for by some aggregates. These aggregates are, as a whole, electroneutral and do not make a forward motion in the electric field.
- o0035 3. The acts of the coagulation (approach and sticking) of various objects: aggregate with aggregate; aggregate with particle; aggregate with wall covered by previously deposited aggregates and resulting “tendrils.” In all cases, there occur both the accelerated movement of a fever massive object and the sticking of a given orientation. Interpretation: the accelerated movement is due to the Coulomb force; orientation is provided by distributed charges.
- p0300 The above phenomena have been repeatedly illustrated by video record frames [65–67, 69,70], omitted here.
- p0305 A quantitative treatment of the characteristics of aggregate movement in electric field allowed us to estimate the electric charges of the aggregates. Most of the particles-aggregates have a charge with the number of positively and negatively charged particles being almost the same. The distribution of particles by charge may be approximated in terms of the Gaussian function, which is symmetric relative to a zero charge. The characteristic charge of the aggregate composes several elementary units. It is worth noting that the charge values are estimated using an average size determined by electron microscopy ($R \approx 1.13 \mu\text{m}$ at aggregate age of 6 min, see Figure 9), and assuming the Stokes drag force law.
- p0310 The X-ray phase analysis indicates that the crystal structure of the spherules, formed in combustion of aluminum particles, is the α and γ phases of Al_2O_3 . For analysis we used: (a) the samples collected by means of a thermophoretic precipitator, and the electron microscope, operating in electronogram recording mode; (b) the samples collected by a vacuum sampler on substrates, and a powder XRD analyzer; and (c) the samples collected on the Petryanov filters. In this case, a filter fragment, cut out with scissors, was used “as is” in the XRD analyzer.

s0090 4.2 Titanium Oxide TiO_2

- p0315 Let us first specify the terminology. In the literature, the nanosized particles, produced by decomposition of a titanium-containing precursor (e.g., TiCl_4) with a subsequent oxidation of Ti clusters in the flame of a gas burner, are usually called the TiO_2 particles,

synthesized by combustion [77]. There is a large body of work, see review [78], devoted to the traditional methods of synthesis of photocatalytic TiO₂, including the above synthesis in a burner. These works commonly describe the authorized method of synthesis (reagents, process organization), the properties of produced TiO₂ particles (size, the specific surface and morphology of particles, the size of crystallites and the regions of coherent scattering, the phase composition, photocatalytic activity), and compare the activities of the resulting particles with the commercial catalysts Degussa P25 or Hombikat.

p0320 In the present work, when discussing the TiO₂ particles produced in combustion, we imply the combustion products of *metallic* titanium microparticles.

p0325 As shown in the introduction, of particular interest are the photocatalytically active TiO₂ particles of nanometric size range and their ability to decompose organic substances. Therefore, we first present general information on the properties of the particles, obtained by conventional methods, to compare them with the particles-products of metallic titanium combustion.

p0330 The TiO₂ nanoparticles are spherical (less often, polyhedral or cubic [79]) and like the primary Al₂O₃ nanoparticles, they are called *spherules*. Their diameter does not usually exceed 100 nm. This size is not the size “natural limit,” but results from the striving of researchers for producing particles as small as possible to obtain the largest specific photocatalytic surface. It is readily proved that on the surface of TiO₂, any organic substances, including live cells, bacteria, and viruses, may be oxidized to CO₂, H₂O, and inorganic residues. The crystal structure of TiO₂ nanoparticles (the main forms, rutile and anatase) has affects the photocatalytic properties, but the data on this influence are rather contradictory. Numerous studies (see reviews [80,81]) are devoted to the doping of particle surface by various metals and nonmetals to increase the quantum yield of decomposition (i.e., photocatalysis efficiency) by broadening the functioning range for the wavelengths of solar light (it is desirable to shift the edge of absorption band to the visible region).

p0335 Let us discuss the characteristics of the combustion products of metallic titanium microparticles. The condensed combustion products are the residues of burning particles, fragmentation products, oxide particles-products of fragment burning mainly in the heterogeneous regime, as well as the highly disperse oxide particles that are either the products of burning in the vapor-phase regime or the condensation products (in particular, spherules). The listed types of the particles-products have been studied in Refs [25,58–65,74,75] (our works) and in Refs [21] and [82] (other authors).

p0340 The evolution of Ti particles of a mean size of $\approx 4 \mu\text{m}$, moving in a plasmotron chamber for tens of milliseconds, was first studied in Ref. [82]. The residual particles were treated according to their morphology as metallic and oxide particles. Besides, the oxide particles (anatase) smaller than 100 nm were revealed, which allowed the authors [82] to assume a combined heterogeneous plus vapor-phase regime of Ti particles combustion.

- p0345 In Ref. [21], devoted to the synthesis of oxide particles upon combustion of metal microparticles in a gas-disperse jet, the data on Al_2O_3 are presented along with those on the TiO_2 spherules formed in combustion of Ti. The synthesis conditions are as follows: primary Ti particles of $\approx 5 \mu\text{m}$; oxygen concentration, 40%; particles concentration, 10^{12} m^{-3} ; and temperature in the jet, 3000–3100 K. The characteristics of synthesized oxide are the following: mean arithmetic diameter, 40 nm; and standard deviation, 16 nm. The size distribution of particles is lognormal with the following parameters: median, 38 nm; mode, 35 nm; and width, 0.38. For parameter definitions, see Section 4.1. The oxide parameters are observed to depend slightly on input conditions (concentration and initial particle size) upon realization of a stable aerodisperse flame. The authors [21] assert that an increase in oxygen concentration above 40% (with a constant concentration of Ti particles of 10^{12} m^{-3}) causes a substantial increase in the yield of TiO_2 nanoparticles, which reaches tens of percent by weight due to the change in combustion regime from heterogeneous to gas phase with a heterogeneous formation of suboxides and their subsequent, additional oxidation in the vicinity of the particle surface. Thus, in this case, the intensification of combustion process favors the formation of nanoparticles. For the general case, this leads to higher temperatures in the reaction zone and the size and properties of the resulting particles-products depend considerably on subsequent cooling.
- p0350 Consider now our data on the combustion products of metallic titanium particles, first of all, on the particle size, structural, crystal, and electrophysical characteristics of oxide TiO_2 nanoparticles.
- p0355 Various experiments were performed using both the different methods of “generation” of burning titanium particles and the different sampling techniques. We present the main experimental techniques.
- o0040 1. The burning of 1-g specimens of chlorine-free compositions, containing 15–29% metallic titanium, ammonium nitrate, and an energetic matrix binder [25,75] in a 20-L vessel, filled with aerosol-free air. The primary titanium particles were of irregular, “spongy” form with sizes less than $100 \mu\text{m}$ (the particles smaller than $63 \mu\text{m}$ contribute 88% of the mass). The composition of plasticine consistency was used either to fill small cups or to obtain specimens of specific form (e.g., conic). The initial titanium particles agglomerated in the combustion wave of the composition. The set of burning particles manifests a wide size distribution, i.e., from the size of the primary particles, introduced in the composition, to the agglomerates of several tens of microns. The size distribution of particles changes with varying fraction of titanium in the composition. Upon combustion of the composition inserted in a small cup 1 cm in diameter, the smallest particles burn out in the flame of the composition while the large ones burn in the air. A certain time after sample combustion (within 0–10 min), the smoke-like aerosol is collected from the vessel onto the thermoprecipitator. The information obtained concerns

- aggregate morphology and spherule size. The aerosol is also sampled in the video microscopy cell to study the motion, coagulation, and charge properties of the aggregates.
- o0045 2. The burning of the gram specimens of the same compositions having the conic form with a base of 1 cm in air. The aerosol is sampled just from the specimen flame with a vacuum sampler (Figure 4). We obtain information on spherule sizes.
- o0050 3. The burning of the gram specimens of the same composition in small cups 1 cm in diameter in a blow-through vessel [30] in the air stream. The particles are sampled on the stack of metallic sieve screens, the Petryanov filter, and the lining covering the surface of the vessel. The time of particle movement from specimen to extinction/sampling location is less than 1 min. We get information on particle distribution within the entire size range, including the smoke fractions with particles smaller than 5 μm .
- o0055 4. The ejection of single burning particles of 100–350 μm from a horizontal quartz capillary with an inner diameter of 2.5 mm [71]. Before experiments, the capillary is loaded with a mixture of ammonium perchlorate (AP) and polymer binder with Ti particles. The particles fly out from the capillary at a speed of 1.5–2 m/s. The glass plate, covered with Formvar film on which the oxide aerosol, formed in combustion, is deposited thermophoretically, is installed at a small angle to the trajectory of particle movement. The deposited particles are then studied under the electron microscope. The method provides information on spherules at the early stage of their growth (at age of 0.1 ms).
- o0060 5. The combustion of monodisperse particles in a vertical 10-L vessel 84 mm in diameter and about 2.4 m in height. The particles used were of two types: (1) A narrow-sieved fraction of spongy-shaped particles with a characteristic size of 38 μm . The fraction was extracted using precision sieve screens with a mesh aperture of 36 and 40 μm . (2) The agglomerates formed of tiny inclusions. The diameter of the agglomerates was 320 μm . A mixture for agglomerate formation consisted of 69% titanium powder (Russian commercial sort “PTM,” 85% of the mass included particles smaller than 50 μm) and polymeric, active binder based on methylpolyvinyl-tetrazole. To realize the ignition and ejection of agglomerates, we used a nonmetalized composition matrix, consisting of 23% AP, 50% HMX (all particles smaller than 10 μm), and 27% binder [61]. This composition was of plasticine consistency. The specimens were in the form of small cylinders, filled either with a metal-free matrix with inserted metalized inclusions, agglomerate “seeds” (Figure 6, position 2), or single 38- μm particles. In experiments, the latter were placed in the nonmetalized matrix in an amount of less than 0.1% and carefully separated from each other. The combustion of 38- μm particles was completed just in the flame of the specimen. The combustion of 320- μm agglomerates continued upon their movement in the air. Experiments on the 38- μm particles and 320- μm

agglomerates were carried out both under ordinary conditions (sample combustion in a small cup in air, combustion of agglomerates in free fall mode) and using a chamber with a nozzle (Figure 6). In the last case, the maximal trajectory–mean velocity of particle movement relative to gas reached 7.9 m/s. These experiments are discussed below. Earlier experiments [23,60], using a chamber with a nozzle, were performed on the specimens of compositions, consisting of 14% Ti powder, that generated polydisperse agglomerates.

p0385 In all the cases, the smoke aerosol was sampled from the vessel with a thermoprecipitator, and the data were obtained on aggregate morphology and spherule size.

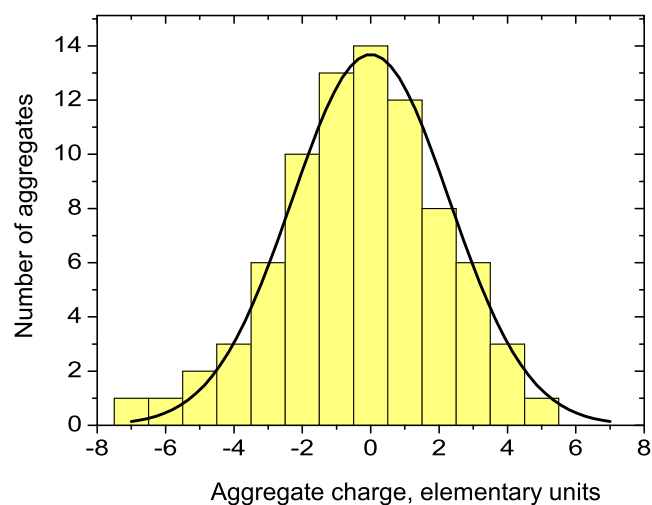
p0390 The experimental results indicate the following.

p0395 The aerosol particles of oxide TiO_2 smoke, like the Al_2O_3 particles, are the chain-branched fractal aggregates of 0.1–10 μm , consisting of spherules of 5–150 nm. Most of the aggregates have either a positive or a negative charge (Figure 11).

p0400 It has been established that the charge distribution of the TiO_2 particles is wider than the equilibrium Boltzmann one at room temperature by a factor of 1.4–3 (the so-called “over equilibrium” one). When the polarity of external electric field is switched, some large-size aggregates of titanium oxide rotate through 180° as the aluminum oxide aggregates. These are the dipoles, i.e., they carry the distributed charges.

p0405 The X-ray phase analysis indicates that the smoke particles represent TiO_2 in the crystal forms of rutile, anatase, and brookite.

p0410 Despite the similarities between the Ti and Al combustion products in the characteristic size of spherules and aggregate morphology, there is a significant distinction in the combustion behavior of these metals. For Al, the size of Al_2O_3 spherules depends on the

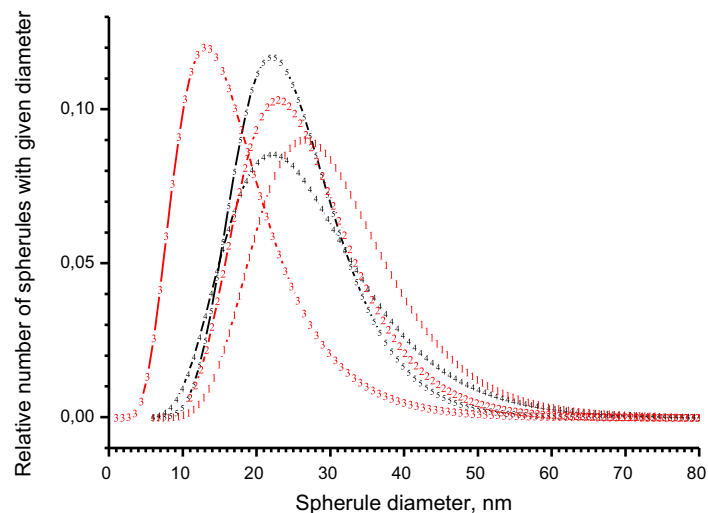


f0060

Figure 11 Distribution of TiO_2 aggregates by values of electric charges [74].

diameter of the burning mother particle. The arithmetic mean diameter, D_{10} , of spherules increases with the size of burning particles and amounts to 17, 51, and 68 nm, respectively, for Al particles of 4, 110, and 340 μm , see [Figure 10](#) and Ref. [57]. This actually allows one to control the size of spherules, which is practically impossible for Ti because the size of spherules is almost independent of the size and burning conditions of Ti particles. Thus, in all our experiments, except for the chamber with a nozzle, the same diameter of the TiO_2 spherules was determined, $D_{10} \approx 23$ nm. We have varied the formulation of gasifying pyrotechnical compositions (in particular, we used the solid oxidizers of four types—ammonium perchlorate, ammonium nitrate, hydrazine mononitrate, and HMX), the size, shape and “origin” of burning particles sizes (sizes from <20 μm to 300 μm ; spongy irregular particles and spherical agglomerates, including monodisperse particles of ≈ 38 μm and monodisperse agglomerates 320 μm in diameter, the polydisperse agglomerates of a size up to 1000 μm), and combustion environment (typically small particles burn in the gaseous products of either pyrotechnical composition, solid propellant, or nonmetalized matrix, and the large ones burn in the air beyond the flame). The fractal dimension of the TiO_2 aggregates was constant, $D_f \approx 1.55$.

p0415 A conservative character of the TiO_2 smoke properties makes it actual to search for the ways to control the parameters of the resulting oxide nanoparticles. These include the effect on the processes of nucleation and condensation via introduction of admixtures (experimentally confirmed for Al_2O_3 in Ref. [21]) as well as the intensification of particle burning. The latter can be realized either by increasing oxygen concentration [21] or by blowing the burning particles. In Ref. [26], we have assumed that the size of spherules depends on the velocity of the burning Ti particle, moving relative to a gaseous medium (the same as blowing the motionless particle). A tiny chamber with a nozzle has been proposed ([Figure 6](#)) for imposing high velocities to the burning particles. The effect of blowing was registered at the qualitative level, but its quantitative description was difficult. In particular, the particle’s velocity for actually polydisperse population was estimated very roughly. Therefore, there was a need to carry out more correct experiments on monodisperse particles. In Refs [60,63,64], quantitative experiments were performed on the monodisperse Ti particles of agglomeration origin of a diameter of 320 μm and with a narrow-sieved particle fraction of about 38 μm . Processing the TEM images of sampled smoke particles provided the size distribution functions of nanometric particles-spherules ([Figure 12](#)). It has been established that an increase in the velocity of particle movement relative to gas leads to a decrease in spherule size. This effect was observed only with the highest (in our experiments) particle blowing velocity, which indicates its threshold character. For the particles 320 μm in diameter, an increase in the trajectory-averaged particle-gas relative velocity from 0.9 to 7.9 m/s causes a decrease in the spherule diameter D_{10} from 28–30 nm to 19 nm; see the table within the legends to [Figure 12](#).



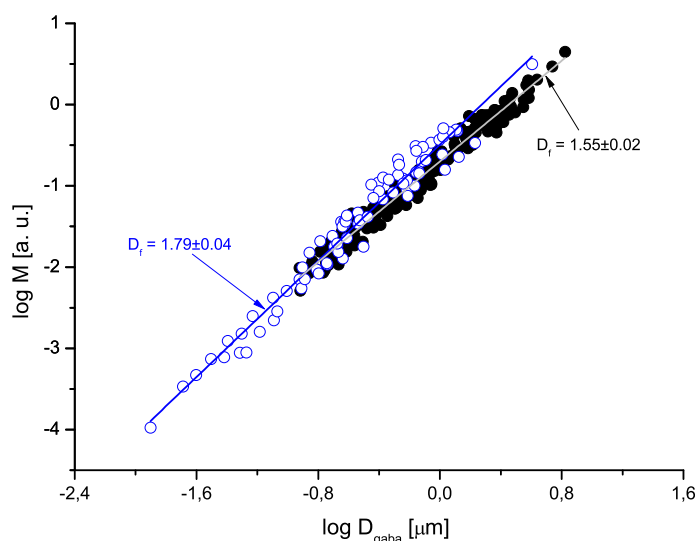
f0065 **Figure 12** Comparison of approximating size distribution functions of spherules [60,63,64].

p0420

t0010

Curve labels	1	2	3	4	5
Initial size of burning particles	320	320	320	38	38
D_0 , micron					
Nozzle, diameter in mm	No nozzle	2	1.5	No nozzle	2
Average (over the burning time) velocity of particle movement relative to gas, cm/s	92	568	789	17	7.5
<i>Statistical parameters of spherules size distribution calculated via treating histograms</i>					
Arithmetic mean diameter D_{10} , nm	30	28	19	29	25
Sd—standard deviation	Sd = 9	Sd = 10	Sd = 10	Sd = 12	Sd = 7
Se—standard deviation of the mean	Se = 0.3	Se = 0.3	Se = 0.1	Se = 0.2	Se = 0.1
The number of measured particles N	860	1458	6056	2743	2687

The movement of the burning Ti particles affects the morphological parameters of oxide aerosol, in particular, causes an increase in the fractal dimension of aggregates up to $D_f = 1.79$, Figure 13. The plot reproduced from Ref. [26] illustrates the procedure for determining the fractal dimension from the slope of the $M(D_{gaba}^{D_f})$ line graph. Here, D_{gaba} is the “conventional diameter” of aggregates equal to the doubled “conventional radius” $R = 0.5\sqrt{LW}$, i.e., $D_{gaba} = 2R$. The hollow circles are the data [26], obtained with blowing; the solid circles are the data [25,74], obtained without blowing. The evaluated maximal blowing velocity is about 10–15 m/s. This rough estimate was obtained from a video record as the length of visible particle tracks divided by frame



f0070 **Figure 13** The effect of particle-gas relative motion of burning particles on the fractal dimension of aggregates [26]. ●—data [25,74] without blowing, ○—data [26] with blowing.

exposure time. It is difficult to present an exact value due to the essential polydispersity of the burning agglomerate set in experiments [26]. The other morphological peculiarities of combustion products for the particles under blowing are the presence of comparatively large particles (up to 300 nm) and mainly rectilinear chains of spherules in aggregate structure. The presence of large particles in the aggregates is, probably, due to the fact that the blowing may lead to a strong fragmentation of burning particles. The fragments burn rapidly in the heterogeneous regime to give comparatively large particles-products (residues). In addition, the burning time of 320- μm agglomerates was recorded to decrease from 0.45 to 0.26 s with increasing blow velocity from 0.9 to 7.9 m/s [64]. The rectilinear spherule chains appear owing to the charge effects and Coulomb interaction. The “high compactness” of the aggregates formed under blowing (verified by higher fractal dimension) is imposed by the presence of large particles whose mass may amount to 0.8 of the aggregate mass [26].

p0430 Thus, the blowing of the burning Ti particles may be considered as a method for intensifying combustion process and for affecting the burning parameters and the characteristics of the nanoparticles formed. It is important to note that the method is of purely physical nature and needs no admixtures.

p0435 Finally, we discuss the data of X-ray phase analysis. The crystal structure of TiO_2 spherules sampled by thermoprecipitator is anatase (60% wt) and rutile (40% wt). The smoke particles sampled on the AFA filter are predominantly of crystal rutile form, and the size of crystallites is 60–80 nm. There are also unidentified reflexes.

p0440 The meagre experimental data [83,84] on the photocatalytic activity of the TiO_2 particles, formed in combustion of metallic Ti, suggest that the TiO_2 aerosol cloud may be used as countermeasures against the local emission of contaminants.



s0095 5. CONCLUSIONS AND FUTURE WORK

p0445 The data available show that the charging of particles due to thermoelectron emission plays a key role in oxide particles formation. The generality of the mechanism accounts for structure similarity and for the closeness of many parameters, describing the properties of aerosol Al_2O_3 and TiO_2 systems. Schematically, the evolution of oxide aerosol may be presented as follows. First, a spherule forms and starts growing due to nucleation and condensation at some distance from the burning particle. Within the condensation zone, the growth of oxide particles proceeds through coalescence. The temperature of spherules decreases with distance from the particle. When it drops below the temperature of oxide melting, the spherules crystallize. The coalescence of liquid particles is replaced by the merging of solid particles into aggregates. Later, already far away from the burning particle, the aggregates may combine and change their structure (e.g., to roll in more compact unit). The forces of electrostatic interaction take part in spherule aggregation, coagulation, and restructuring.

p0450 Finally, we can state that in studies on oxide nanoparticles formation in combustion of Al and Ti particles, progress was made toward the characterization of particle size and morphology. Some problems, however, remain unresolved.

p0455 Note that the formation of nanoparticles is one of the essential features of the mechanism of metal particles combustion. This mechanism includes the transport of reagents to the reaction zone, i.e., oxidizer from the environment, and/or particle substances (primary metal vapor, suboxides or oxides). A concrete realization of these processes greatly affects the number and properties of nanoparticles. The interaction between the macrokinetics of the initial metal consumption and the formation of dispersed oxide may be considered as the major task for future investigations. For nanosized oxide particles, the following particular problems can be formulated. At what stage of mother particle combustion are they formed? What is the actual mechanism? How can it be intensified?

p0460 For aluminum, there are the answers to the first two questions. The nano-oxide particles form from either the vapor-phase oxidation of metals or the oxidation of suboxides, evaporated from the burning particle and delivered into the reaction zone above the burning particle surface. Unsolved is the problem of the intensification of Al_2O_3 nanoparticles formation. In particular, it is of interest to explore whether the blowing of Al particle may have any effect. What will happen after a decrease in the size of burning particles, e.g., down to the size of submicron particles?

p0465 For titanium, the first two questions have not yet been answered. As for the third question, it has been established that the formation of nanoparticles may be intensified via air blowing (in particular, the spherule size may be reduced). An intense evaporation may occur at an early stage with oxidation reaction proceeding in the kinetic regime. Of interest is a further increase in particle-gas velocity, i.e., the existence of blowing effect “scale.” An important problem of the mechanism of titanium particles combustion is the particles fragmentation, and its feasible application for intensifying combustion and for increasing the yield of nanoparticles. Of interest may also be the search for admixtures (e.g., other metals) that may favor the destruction of the oxide layer. Finally, further study of the photocatalytic properties of nanoparticles formed in Ti particles combustion is also needed.

ACKNOWLEDGMENTS

The authors are grateful to all the coauthors and colleagues of the ICKC SB RAS with whom they had fruitful discussions for a number of years. V.E.Z. thanks the Ministry of Education and Science of the Russian Federation for partial financial support within the framework of the Federal Target Program. Agreement No. 14.578.21.0034 (RFMEFI57814X0034).

s0100 REFERENCES

- [1] P.F. Pokhil, A.F. Belyayev, Y.V. Frolov, V.S. Logachev, A.I. Korotkov, *Combustion of Powdered Metals in Active Media*, Nauka, Moscow, 1972 (in Russian). Also available in English: FTD-MT-24-551-73, translated by National Technical Information Service, 1973, pp. 1–395.
- [2] V.E. Zarko, O.G. Glotov, Formation of Al oxide particles in combustion of aluminized condensed systems (review), *Sci. Technol. Energ. Mater.* 74 (6) (2013) 139–143.
- [3] The Treaty between the United States of America and the Union of Soviet Socialist Republics on the Elimination of Their Intermediate-range and Shorter-range Missiles, December 8, 1987.
- [4] V.V. Adushkin, S.I. Kozlov, A.V. Petrov (Eds.), *Environmental problems and risks of impact of the missile and space equipment on environment*. Handbook, Ankil, Moscow, 2000, 640 pages (in Russian).
- [5] A.S. Zharkov, M.G. Potapov, G.A. Demidov, G.V. Leonov, *Bench Tests of the Solid Propellant Energetic Devices*, Altai State Technical University Press, Barnaul, 2001, 281 pages (in Russian).
- [6] L.V. Zabelin, R.B. Gafiyatullin, L.R. Guseva, Environmental aspects of problem of utilization of charges of solid-propellant rockets, *Chemistry in Russia* 2 (1999) 4–7 (in Russian).
- [7] D.P. Samsonov, V.P. Kiryukhin, N.P. Zhiryukhina, R.I. Pervunina, Determining polychlorinated dibenzo-*n*-dioxins, dibenzofurans, biphenils, and polynuclear aromatic substances in combustion products of solid rocket propellant, *J. Anal. Chem.* 51 (1996) 1218–1221 (in Russian).
- [8] A.M. Lipanov, M.A. Korepanov, Z.A. Tuhvatullin, Experimental and theoretical study of formation of toxic compounds in the process of utilization of complex chemical substances, *Bull. Izhevsk State Tech. Univ.* (2) (2003) 51–54 (in Russian).
- [9] S.E. Pashchenko, V.E. Zarko, B.D. Oleinikov, S.M. Utkin, T.B. Tihomirova, S.P. Vlasova, Qualitative Analysis of Basic Processes Taking Place in Formation and Propagation of the Superfine Aluminium Oxides Aerosols from Open and Bench Firing the Large-size Solid Propellant Motors and Methods of Their Study/Problem Questions of Methodology of Utilization of Solid Rocket Propellants, Wastes and Reminders of Liquid Rocket Propellants in the Elements of Missile and Space Equipment, Joint Stock Company Federal Research and Production Center “Altai” Press, Biysk, 2000 (in Russian) p. 133–143.

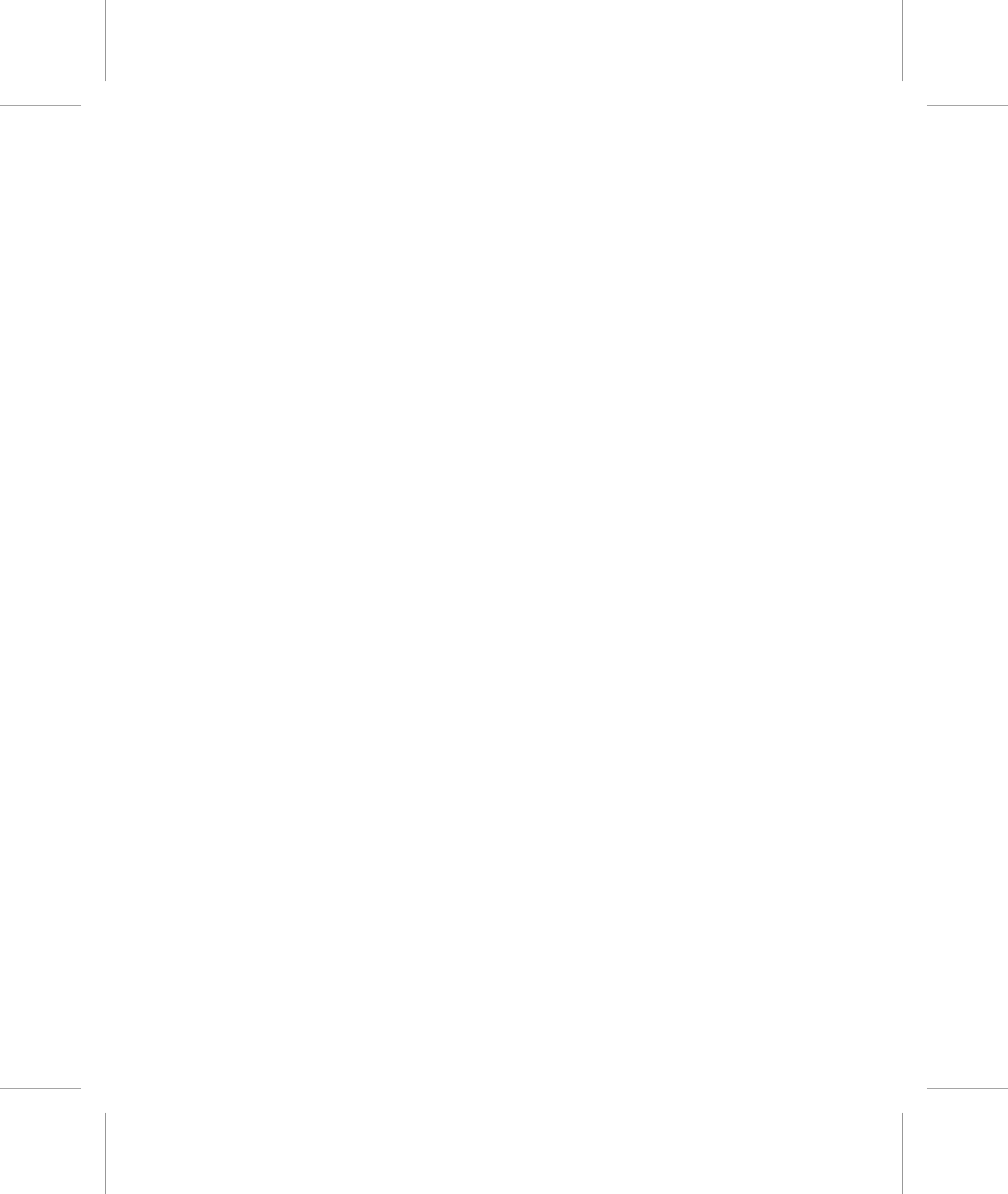
- [10] V.I. Romanov, Accident of the solid propellant rocket on a launching site, *Cosmic Res.* 34 (12) (1996) 102–105 (in Russian).
- [11] A.M. Lipanov, M.A. Korepanov, Z.A. Tuhvatullin, Study of formation of the polychlorinated aromatic hydrocarbons upon the solid rocket propellant utilization, *Chem. Phys. Mesoscopy* 9 (1) (2007) 15–26 (in Russian).
- [12] S.I. Burdyugov, M.A. Korepanov, N.P. Kuznetsov, Utilization of Solid Propellant Rocket Motors. Rocket Production Series, Space Research Institute Press, Moscow, 2008, ISBN 978-5-93972-657-3 (in Russian).
- [13] V.I. Romanov, Applied Aspects of Accidental Atmospheric Emissions. Handbook, Fizmatkniga, Moscow, 2006, 368 pages (in Russian).
- [14] L.A. Fedorov, Dioxines as Ecological Hazard: Retrospectives and Perspectives, Nauka, Moscow, 1993 (in Russian).
- [15] B.I. Vorozhtsov, A. Galenko Yu, V.P. Lushev, V.I. Mar'yash, B.D. Oleinikov, A.A. Pavlenko, M.G. Potapov, Yu V. Khrustalev, B.M. Bashunov, Experimental investigations of the spread of products from industrial explosive combustion, *Atmos. Oceanic Opt.* 10 (6) (1997) 425–431, 681–686.
- [16] V.G. Ivanov, S.N. Leonov, G.L. Savinov, O.V. Gavrilluk, O.V. Glazkov, Combustion of mixtures of ultradisperse aluminum and gel-like water, *Combust. Explos. Shock Waves* 30 (4) (1994) 569–570.
- [17] A.A. Gromov, T.A. Habas, A.P. Il'in, et al., Combustion of Nano-sized Metal Powders, Deltaplan Press, Tomsk, 2008, 382 pages (in Russian).
- [18] A.P. Il'in, A.A. Gromov, Combustion of Ultra-fine Aluminum and Boron, Tomsk State University Publ, Tomsk, 2002, 154 pages (in Russian).
- [19] D.A. Yagodnikov, Ignition and Combustion of Powder Metals, The Bauman University Publishing House, Moscow, 2009, ISBN 978-5-7038-3195-3 (in Russian).
- [20] K.A. Yu, Adaptation of the Inside-chamber Processes and Elements of the Energetic Installation Utilizing Powder Fuel to Technologies for Obtaining Ultra- and Nanodispersed Materials, Perm national research polytechnic university Press, Perm, 2012, ISBN 978-5-398-00725-1, 236 pages (in Russian).
- [21] N.I. Poletaev, A.N. Zolotko, Y.A. Doroshenko, Degree of dispersion of metal combustion products in a laminar dust flame, *Combust. Explos. Shock Waves* 47 (2) (2011) 153–165.
- [22] L.B. Zubkov, Space Metal. All About Titanium, Nauka, Moscow, 1987, 129 pages. (in Russian).
- [23] V. Weiser, J. Neutz, N. Eisenreich, E. Roth, H. Schneider, S. Kelzenberg, Development and characterization of pyrotechnic compositions as counter measures against toxic clouds, in: *Energetic Materials: Performance and Safety. 36th Int. Annual Conf. of ICT & 32nd Int. Pyrotechnics Seminar*, June 28–July 1, 2005, ICT, Karlsruhe, Germany, 2005, pp. 102–1–1102–12.
- [24] L.T. DeLuca, L. Galfetti, F. Severini, L. Meda, G. Marra, A.B. Vorozhtsov, V.S. Sedoi, V.A. Babuk, Burning of nano-aluminized composite rocket propellants, *Combust. Explos. Shock Waves* 41 (6) (2005) 680–692.
- [25] O.G. Glotov, V.N. Simonenko, R.S. Zakharov, V.E. Zarko, Combustion characteristics of pyrotechnic mixtures containing titanium, energetic materials, in: *Characterisation and Performance of Advanced Systems. 38th Int. Annual Conference on Energetic Materials – Characterization and Performance of Advanced Systems*, Karlsruhe, Germany June 26–29, 2007, pp. 87–1–987–15. Also Available in Russian: R.S. Zakharov, O.G. Glotov, Combustion characteristics of pyrotechnic compositions containing powdered Ti//*Bulletin of Novosibirsk State University, Physics Series*, 2 (3) (2007) 32–40, http://www.phys.nsu.ru/vestnik/catalogue/2007/03/Vestnik_NSU_07T2V3_p1-103.pdf.
- [26] O.G. Glotov, V.E. Zarko, V.N. Simonenko, A.A. Onischuk, A.M. Baklanov, S.A. Gus'kov, A.V. Dushkin, In search of effective ways for generation of TiO₂ nanoparticles by means of firing Ti-containing pyrotechnic composition, in: *EUCASS 2009, 3rd European Conference for Aerospace Sciences*, France, Paris, July 6–9, 2009, ISBN 978-2-930389-47-8. M.L. Riethmuller, Editor-in-Chief. CD Copyright 2009 by the von Karman Institute for Fluid Dynamics.
- [27] O.G. Glotov, V.E. Zarko, V.N. Simonenko, A.A. Onischuk, A.M. Baklanov, Size and morphology of the nanooxide aerosol formed in combustion of aluminum and titanium particles in air, in: *Combustion of Solid Fuel, Proceedings of VII All-Russian Conf.* Novosibirsk, 10–13 November, 2009, vol. 3, Kutateladze Institute of Thermophysics Press, Novosibirsk, 2009, pp. 184–190 (in Russian).

- [28] O.G. Glotov, S.E. Pashchenko, V.V. Karasev, Z.V. Ya, V.M. Bolvanenko, Methods for sampling and particle-size analysis of condensed combustion products, in: *Physics of Aerodisperse Systems*, N 30, Vishcha shkola, Kiev–Odessa, 1986, pp. 43–50 (in Russian).
- [29] O.G. Glotov, V.Y. Zyryanov, The effect of pressure on characteristics of condensed combustion products of aluminized solid propellants, *Arch. Combust.* 11 (3–4) (1991) 251–262.
- [30] O.G. Glotov, V.Y. Zyryanov, Condensed combustion products of aluminized propellants. I. A technique for investigating the evolution of disperse-phase particles, *Combust. Explos. Shock Waves* 31 (1) (1995) 72–78.
- [31] O.G. Glotov, V.E. Zarko, V.V. Karasev, M.W. Beckstead, Aluminum agglomeration in solid propellants: formulation effects, in: *Propellants, Explosives, Rockets, and Guns. Proceedings of the Second International High Energy Materials Conference and Exhibit*, December 8–10, 1998, IIT Madras, Chennai, India, 1998, pp. 131–137.
- [32] O.G. Glotov, V.E. Zarko, Agglomeration in combustion of aluminized solid propellants with varied formulation, in: *Proc. of 2nd European Conference on Launcher Technology – Space Solid Propulsion*, Italy, Rome, 2000, 14 pages.
- [33] O.G. Glotov, V.E. Zarko, Condensed combustion products of aluminized propellants, *Trans. AASRC*, 34 (3) (2002) 247–256.
- [34] K. Hori, O.G. Glotov, V.E. Zarko, H. Habu, A.M.M. Faisal, T.D. Fedotova, Study of the combustion residues for Mg/Al solid propellant, in: *Energetic Materials: Synthesis, Production and Application. 33th Int. Annual Conference of ICT*, Karlsruhe, Germany, 2002, pp. 71–71-14.
- [35] I.V. Petryanov, V.I. Kozlov, P.I. Basmanov, et al., *Fibrous Filtering Materials FP, Znanie*, Moscow, 1968 (in Russian).
- [36] O.G. Glotov, V.A. Zhukov, Evolution of 100- μm aluminum agglomerates and initially continuous aluminum particles in the flame of a model solid propellant. Part I. Experimental approach, *Combust. Explos. Shock Waves* 44 (6) (2008) 662–670.
- [37] T.D. Fedotova, O.G. Glotov, V.E. Zarko, Chemical analysis of aluminum as a propellant ingredient and determination of aluminum and aluminum nitride in condensed combustion products, *Propell. Explos. Pyrotech.* 25 (6) (2000) 325–332.
- [38] T.D. Fedotova, O.G. Glotov, V.E. Zarko, Peculiarities of chemical analysis of ultra fine aluminum powders, in: *Energetic Materials. Performance and Safety, 36th International Annual Conference of ICT & 32nd International Pyrotechnics Seminar*. Karlsruhe, Germany. June 28–July 1, 2005, pp. 147-1–147-14.
- [39] T.D. Fedotova, O.G. Glotov, V.E. Zarko, Application of cerimetric methods for determining the metallic aluminum content in ultrafine aluminum powders, *Propell. Explos. Pyrotech.* 32 (2) (2007) 160–164.
- [40] O.G. Glotov, V.E. Zarko, V.V. Karasev, Problems and prospects of investigating the formation and evolution of agglomerates by the sampling method, *Combust. Explos. Shock Waves* 36 (1) (2000) 146–156.
- [41] P.I. Basmanov, V.N. Kirichenko, N. Filatov Yu, Yu L. Yurov, Highly Effective Purification of Gases of Aerosols with Petryanov Filters, Moscow, 2002, 193 pages (in Russian), http://www.electrospinning.ru/userfiles/ufiles/vysokoeffektivnaya_ochistka_gazov_ot_aerozoley_p.i.basmanov_i_dr..pdf.
- [42] J.P. Lodge Jr., T.L. Chan (Eds.), *Cascade Impactor Sampling and Data Analysis*, American Industrial Hygiene Association, Akron, Ohio, 1986.
- [43] Diffusion Aerosol Spectrometer “DSA”. <http://www.kinetics.nsc.ru/results/paper44.html> (in Russian).
- [44] State standard specification of Russia GOST R 8.755–2011. Disperse composition of gas environments. Determination of the sizes of nanoparticles by method of diffusion spectrometry (in Russian).
- [45] A. Ankilov, A. Baklanov, R. Mavliev, S. Eremenko, Comparison of the Novosibirsk diffusion battery with the Vienna electromobility spectrometer, *J. Aer. Sci.* 22 (1991) S325.
- [46] A. Ankilov, A. Baklanov, M. Colhoun, K.-H. Enderle, J. Gras, et al., Intercomparison of number concentration measurements by various aerosol particle counters, *Atmos. Res.* 62 (2002) 177–207, <http://aeronanotechnology.com/d/54311/d/intercalibration.pdf>.

- [47] A.A. Paletsky, A.G. Tereshenko, E.N. Volkov, et al., Study of the CL-20 flame structure using probing molecular beam mass spectrometry, *Combust. Explos. Shock Waves* 45 (3) (2009) 286–292.
- [48] S.E. Pashchenko, V.V. Karasev, Method of sampling of aerosol from flame or nozzle. USSR inventors certificate no. 1186994, *Bull. Invention* (396) (1985) (in Russian).
- [49] E.A. Ershov, S.A. Kambalin, V.V. Karasev, S.E. Pashchenko, Sampling of aerosols for electron-probe analysis by vacuum sampler, *Zavodsk. Lab.* (6) (1992) 31–34 (in Russian).
- [50] D. Gonzalez, A.G. Nasibulin, A.M. Baklanov, S.D. Shandakov, et al., A new thermophoretic precipitator for collection of nanometer-sized aerosol particles, *Aerosol Sci. Technol.* 39 (2005) 1064–1071, <http://dx.doi.org/10.1080/02786820500385569>.
- [51] O.G. Glotov, Image processing of the fractal aggregates composed of nanoparticles, *Russ. J. Phys. Chem. A* 82 (13) (2008) 49–54, <http://dx.doi.org/10.1134/S0012501607030050>.
- [52] O.G. Glotov, Condensed combustion products of aluminized propellants. IV. Effect of the nature of nitramines on aluminum agglomeration and combustion efficiency, *Combust. Explos. Shock Waves* 42 (4) (2006) 436–449.
- [53] O.G. Glotov, V.A. Zhukov, The evolution of 100- μ m aluminum agglomerates and initially continuous aluminum particles in the flame of a model solid propellant. II. Results, *Combust. Explos. Shock Waves* 44 (6) (2008) 671–680.
- [54] G.L. Ya., Guide to the Dispersion Analysis with a Microscopy Method, Chemistry, Moscow, 1979 (in Russian).
- [55] O.G. Glotov, V.V. Karasev, V.E. Zarko, T.D. Fedotova, M.W. Beckstead, Evolution of aluminum agglomerates moving in combustion products of model solid propellant, in: K.K. Kuo, L.T. De Luca (Eds.), *Combust. Energ. Mater.*, Begell House, New York, 2002, pp. 397–406. Also Available in: O.G. Glotov, V.V. Karasev, V.E. Zarko, T.D. Fedotova, M.W. Beckstead, Evolution of aluminum agglomerates moving in combustion products of model solid propellant, *Int. J. Energ. Mater. Chem. Propuls.* 5 (1–6) (2002) 397–406.
- [56] O.G. Glotov, V.E. Zarko, V.V. Karasev, T.D. Fedotova, A.D. Rychkov, Macrokinetics of combustion of monodisperse agglomerates in the flame of a model solid propellant, *Combust. Explos. Shock Waves* 39 (5) (2003) 552–562.
- [57] O.G. Glotov, A.A. Onischuk, V.V. Karasev, V.E. Zarko, A.M. Baklanov, Size and morphology of the nanooxide aerosol generated by combustion of an aluminum droplet, *Doklady Phys. Chem.* 413 (Part 1) (2007) 59–62.
- [58] O.G. Glotov, V.N. Simonenko, V.E. Zarko, G.S. Surodin, Combustion of monodisperse titanium particles in air, in: *Energetic Materials for High Performance, Insensitive Munitions and Zero Pollution*. 41st Int. Annual Conference of ICT, Karlsruhe, Germany, June 29–July 02, 2010, 2010, pp. 30–1–330–14.
- [59] O.G. Glotov, V.E. Zarko, V.N. Simonenko, Combustion of monodisperse titanium particles free falling in air, in: *Energetic Materials: Modelling, Simulation and Characterisation of Pyrotechnics, Propellants and Explosives*. 42nd International Annual Conference of the Fraunhofer ICT, June 28–July 01, 2011. Karlsruhe, Germany, 2011, pp. 45–1–45–12.
- [60] O.G. Glotov, Combustion of titanium particles in air, in: *Proceedings of the International Conference “Modern Problems of Applied Mathematics and Mechanics: The Theory, Experiment and Practice”*, Devoted to the 90 Anniversary since the Birth of the Academician N. N. Yanenko (Novosibirsk, Russia, May 30–June 4, 2011), 2011 (in Russian), http://conf.nsc.ru/files/conferences/niknik-90/fulltext/37173/46861/Glotov_Ti_6pages.pdf.
- [61] O.G. Glotov, Combustion of spherical titanium agglomerates in air. I. Experimental approach, *Combust. Explos. Shock Waves* 49 (3) (2013) 299–306.
- [62] O.G. Glotov, Combustion of spherical titanium agglomerates in air. II. Experimental results, *Combust. Explos. Shock Waves* 49 (3) (2013) 307–319.
- [63] O.G. Glotov, V.N. Simonenko, A.M. Baklanov, O.N. Zhitnitsky, G.S. Surodin, Effect of size and velocity of moving titanium particles on nano-sized aerosol particle characteristics, in: *Combustion of Solid Fuel*. Proceedings of VIII All-Russian Conf., Novosibirsk, 13–16 November 2012, Kutateladze Institute of Thermophysics Press, Novosibirsk, 2012, ISBN 978-5-89017-032-3, pp. 32.1–32.8 (in Russian), <http://www.itp.nsc.ru/conferences/gtt8/files/32Glotov.pdf>.

- [64] O.G. Glotov, Combustion characteristics of monodisperse titanium particles fast moving in air, in: *Energetic Materials: Characterization and Modeling of Ignition Process, Reaction Behavior and Performance*. 44th Int. Annual Conference of the Fraunhofer ICT, June 25–28, 2013. Karlsruhe, Germany, 2013, pp. 61–1–61–14.
- [65] V.V. Karasev, Formation of Nanoaerosol of Oxides of Metal, Silicon and Soot in Processes of Combustion and Pyrolysis, 2006. Abstract of Cand. Sci. thesis (Physics and Mathematics, 01.04.17), Novosibirsk (in Russian).
- [66] V.V. Karasev, S. di Stasio, A.A. Onischuk, A.M. Baklanov, O.G. Glotov, V.E. Zarko, V.N. Panfilov, Synthesis of charged agglomerates of Al_2O_3 particles in a combustion reactor, *J. Aerosol Sci.* 32 (S1) (2001) 593–594.
- [67] V.V. Karasev, A.A. Onishchuk, O.G. Glotov, A.M. Baklanov, V.E. Zarko, V.N. Panfilov, Charges and fractal properties of nanoparticles – combustion products of aluminum agglomerates, *Combust. Explos. Shock Waves* 37 (6) (2001) 734–736.
- [68] B.M. Smirnov, *Physics of Fractal Clusters*, Nauka, Moscow, 1991 (in Russian).
- [69] V.V. Karasev, O.G. Glotov, A.M. Baklanov, A.A. Onischuk, V.E. Zarko, Alumina nanoparticle formation under combustion of solid propellant, in: *Energetic Materials. Synthesis, Production and Application*, 33 International Annual Conference of ICT. June 25–June 28, 2002. Karlsruhe, Germany, 2002, pp. 14–1–214–13.
- [70] V.V. Karasev, A.A. Onischuk, O.G. Glotov, A.M. Baklanov, A.G. Maryasov, V.E. Zarko, V.N. Panfilov, A.I. Levykin, K.K. Sabelfeld, Formation of charged aggregates of Al_2O_3 nanoparticles by combustion of aluminum droplets in Air, *Combust. Flame* 138 (2004) 40–54.
- [71] S.A. Khromova, V.V. Karasev, A.A. Onischuk, O.G. Glotov, V.E. Zarko, Formation of nanoparticles of TiO_2 and Al_2O_3 at combustion of metal droplets, in: G. Roy, S. Frolov, A. Starik (Eds.), *Nonequilibrium Processes, Plasma, Aerosols, and Atmospheric Phenomena*, vol. 2, Torus Press, Ltd., Moscow, 2005, ISBN 5-94588-034-5, pp. 225–234.
- [72] V.V. Karasev, O.G. Glotov, A.M. Baklanov, N.I. Ivanova, A.R. Sadykova, A.A. Onischuk, Formation of soot and metal oxide charged aggregates of nanoparticles by combustion and pyrolysis, in: G. Roy, S. Frolov, A. Starik (Eds.), *Combustion and Pollution: Environmental Impact*, Torus press, Moscow, 2005, ISBN 5-94588-030-2, pp. 207–228.
- [73] V.V. Karasev, A.A. Onischuk, S.A. Khromova, O.G. Glotov, V.E. Zarko, E.A. Pilyugina, C.-J. Tsai, P.K. Hopke, Peculiarities of oxide nanoparticle formation during metal droplet combustion, in: *Energetic Materials. Insensitivity, Ageing, Monitoring*. 37th International Annual Conference of ICT. Karlsruhe, Germany, 2006, pp. 124-1–124-212, <http://www.kinetics.nsc.ru/comp/comp2007/on11.pdf>.
- [74] V.V. Karasev, A.A. Onischuk, S.A. Khromova, O.G. Glotov, V.E. Zarko, et al., Formation of metal oxide nanoparticles in combustion of titanium and aluminum droplets, *Combust. Explos. Shock Waves* 42 (6) (2006) 649–662.
- [75] O.G. Glotov, V.N. Simonenko, A.M. Baklanov, V.E. Zarko, et al., Formation of nano-particles of titanium dioxide by combustion of pyrotechnical composition on basis of mechanoactivated composition of titanium with mono-nitrate of hydrazine, in: *High Energy Materials: Demilitarization, Antiterrorism and Civil Application*. Abstracts of IV International Workshop HEMs–2008 (September 3–5, 2008, Belokurikha), FSUE FR&PC ALTAI, Biysk, 2008, pp. 120–124 (in Russian), <http://frpc.secna.ru/hems/docs/hems-2008.rar>.
- [76] S.K. Friedlander, *Smoke, Dust, and Haze*, Oxford Univ. Press, New York–Oxford, 2000.
- [77] N.K. Memon, D.H. Anju, S.H. Chung, Multiple-diffusion flame synthesis of pure anatase and carbon-coated titanium dioxide nanoparticles, *Combust. Flame* 160 (2013) 1848–1856.
- [78] I.F. Myronyuk, V.L. Chelyadyn, Obtaining methods of titanium dioxide (Review), *Phys. Chem. Solid State* 11 (4) (2010) 815–831 (in Ukrainian), http://www.nbu.gov.ua/portal/natural/Phkhtt/2010_4/1104-03.pdf.
- [79] S. Jöks, D. Klauson, M. Krichevskaya, S. Preis, et al., Gas-phase photocatalytic activity of nanostructured titanium dioxide from flame aerosol synthesis, *Appl. Catal. B: Environ.* 111–112 (2012) 1–9.
- [80] Y.-C. Nah, I. Paramasivam, P. Schmuki, Doped TiO_2 and TiO_2 nanotubes: synthesis and applications, *ChemPhysChem* 11 (2010) 2698–2713, <http://dx.doi.org/10.1002/cphc.201000276>.

- [81] H. Sun, S. Wang, H. Ming Ang, M.O. Tadó, et al., Halogen element modified titanium dioxide for visible light photocatalysis (Review), *Chem. Eng. J.* 162 (2010) 437–447.
- [82] A.P. Dolganov, V.N. Kovalev, V.E. Liepinya, E.I. Shipin, Investigation of the regularities of titanium burning particles in a gas stream, Proceedings of the Academy of Sciences of Latvian the Soviet Socialist Republic, Ser. Phys. Tech. Sci. (Latvijas PSR Zinatnu Akademijas Vestis, Fiz. Tehnisko Zinatnu Ser.) 2 (1990) 106–113 (in Russian).
- [83] Y. Kitamura, N. Okinaka, T. Shibayama, et al., Combustion synthesis of TiO₂ nanoparticles as photocatalyst, *Powder Technol.* 176 (2007) 93–98.
- [84] V.S. Zakharenko, V.N. Parmon, S.A. Khromova, Chemical and optical properties of the titanium dioxide produced from combustion of titanium microparticles in air, *Atmos. Oceanic Opt.* 20 (6) (2007) 486–491.



Abstract

The necessity and practical importance of studying the characteristics of oxide nanoparticles formed in combustion of aluminum (Al) and titanium (Ti) microparticles are substantiated. Experimental techniques and results are reviewed. Priority is given to the methods developed at the Institute of Chemical Kinetics and Combustion and to the original results obtained by these methods. It is shown that despite distinctions in the mechanisms of aluminum and titanium combustion, the oxide nanoparticles, Al_2O_3 and TiO_2 , are of almost the same dimensions and display similar morphological and charge properties. Future investigations should be concerned with a mutual influence of the macrokinetics of the consumption of active particle metal on the formation of disperse oxide. The problems of high priority are formulated.

Keywords:

Al; Chain-branched aggregate; Combustion; Electric charge; Fractal dimension; Nanoparticles; Oxide formation; Size distribution; Spherules; Ti.